Experimental Studies of Gas-Phase Main-Group Metal Clusters

MANFRED M. KAPPES

Department of Chemistry, Northwestern University, Evanston, Illinois 60204

Received April 8, 1987 (Revised Manuscript Received July 14, 1987)

Contents

Manfred M. Kappes was born in Bonn, West Germany, in 1957. Following undergraduate studies at Concordia University in Montreal (B.Sc., 1977) he continued his chemistry education at MIT (Ph.D., 1981). After a postdoctoral sojourn in the group of E. Schumacher in Bern, Switzerland, and subsequent Habilitation (1987), he moved to Northwestern University where he is now Assistant Professor of physical chemistry. His research interests encompass experimental studies of temperature and structure and phase in gas-phase metal microclusters as well as the characterization of model catalysts via deposition of size-selected aggregates onto surfaces and into matrices.

1. Introduction

1.1. Semantics

The subjects of this review are neutral clusters (M_x, $2 < x < 100$) composed of main-group metals (particularly group 1a). We distinguish between bare and ligated clusters and after briefly discussing the latter will concentrate on experimental studies of the former. Bare clusters are extremely reactive and as such their characterization poses a number of experimental problems. Two general approaches are being presently used: (a) collisionless supersonic beams and (b) deposition into, or in situ production in, inert-gas matrices. While also considering aspects of matrix studies, this paper is devoted to gas-phase measurements in which particle specificity is ensured and cluster-support interactions that may influence equilibrium structures by charge transfer/epitaxy are absent.

Subdivision of the field of metal clusters among main-group metal and transition-metal species is somewhat arbitrary: many of the cluster size effects observed for aggregates of transition metals are paralleled by main-group metal clusters, which are significantly easier to describe theoretically. It has developed that an understanding of size effects in main-group metal clusters is indispensable for a coherent picture of bonding in transition-metal species. Therefore, while this review will concentrate on those clusters of main-group metals for which we have experimental data (Li, Na, K, Rb, and Cs and to a lesser extent Al, Pb, Bi, In, Mg, Ca, Ba, and Sr), we will also consider relevant aspects of transition-metal cluster studies wherever necessary.

The properties of small bare metal clusters are dominated by an atomic coordination very different from

0009-2665/88/0788-0369$06.50/0

crystalline bulk and from that expected on the basis of chemical valence. Compact structures are encountered with high surface to volume ratios. This can be best appreciated by considering as an example of highly coordinated, spheroidal structures the series of consecutive shell Mackay icosahedra:[1] 13, 55, 147, ..., atoms, for which the corresponding surface to bulk atom number ratios are 12, 3.23, and 1.673, respectively.

On going from the molecular to bulk metallic limit, we expect metal clusters to manifest large, discontinuously size dependent variations in physical and chemical properties due to both the influence of packing (most stable = densest packing?) and electronic structure (extensively delocalized orbitals but a finite number of atoms). Such variation is obviously dependent on the property in question, and *its elucidation is the goal of cluster research.* Note that, in many cases, the property itself becomes ill-defined at either the macroscopic or microscopic limit (e.g. surface area, surface tension, superconductivity[2]). There may in fact be observables adequately describing the intermediate cluster size regime that are not applicable to either size limit (e.g., equilibrium structures consistent with icosahedral habit rather than bulk lattice).

The question of the most interesting size range for study arises. A purely classical approach suggests that, for mercury clusters, per unit area surface free energy, enthalpy, and entropy come within 5% of bulk values for 40, 36, and 6 atoms, respectively.[3] Of course quantum chemical calculations on these clusters at much higher levels of sophistication would come to quantitatively different conclusions.[4] However, the general consensus is that many chemically interesting properties reach values within a few percent of their bulk limits at about M_{100}. Most others can at this point be classically extrapolated to their corresponding solid state values by assuming spherical clusters and taking into account curvature and surfact tension. For example "one-electron" observables such as ionization potential or electron affinity go as $N^{-1/3}$. Consequently *largest, cluster size dependent variations in physical and chemical properties are thought to occur below* M_{100}.

1.2. Bare versus Clothed Clusters

Due mainly to experimental factors, we still have little particle-specific experimental information over large size ranges on *bare* metal cluster properties, excepting ionization potentials, polarizabilities, electron affinities, and chemical reactivities; see below. Therefore, why not study cluster complexes for which experimental data are more readily accessible.

In contrast to bare clusters, synthesis of multi-metal complexes surrounded by a coating of weakly bound organic ligands is now almost routine. The largest yet made contains 520 Pd atoms[5] according to electron microscopy, which shows a support covered uniformly with 20-Å icosahedral objects. Cluster complexes are generated monodispersed and typically in large amounts (>10^{21}). While often air- and water-sensitive, they are not nearly as reactive as bare metal clusters and can be probed at relative leisure with the entire arsenal of inorganic analysis methods. The many compounds made and crystal structures determined[6] [e.g., $(Ni_{38}Pt_6(CO)_{48}H_2)(NEt_4)_2$] have allowed the formulation of bonding rules via the observation of preferred electron counts (magic numbers) and geometries.[7] These rules appear to have many exceptions. Note that, for larger complexes, typical synthesis routes involving removal of one or two ligands from smaller complexes and growth through these centres of coordinative unsaturation lead to ligated clusters whose central metal core exhibits vertex, face, or edge sharing and perhaps not the thermodynamically most stable configuration.

Clothed clusters were originally studied in part because they were thought to represent models for chemically modified metal surfaces.[8] More recently it has been proposed that their structural and chemical properties are closely related to those of the corresponding bare metal cluster species.[9] Both assumptions have proved erroneous in $M_x(lig)_y$ ($x < 50$) due to the magnitude of ligand effects. This is demonstrated most impressively by measurements of magnetization and magnetic susceptibility[10] for Pt and Ni complexes. These show (a) small but finite magnetic moments in various $Pt_x(lig)_y$ species [e.g., $(Pt_{38}(CO)_{44}H_2)(PPN)_2$] in contrast to the zero moment expected on the basis of diamagnetic bulk and the atomic closed-shell electron configuration and (b) much smaller per atom moments in $Ni_x(lig)_y$ [e.g., $(Ni_{34}(CO)_{38}CH)(NEt_4)_5$] than found in ferromagnetic bulk or predicted by calculations of bare nickel clusters that yield highly degenerate ground states with associated large multiplicities. These deviations can be qualitatively rationalized in terms of the low spin, nearly closed-shell electron configurations associated with coordinative saturation as has been shown in a series of ab initio calculations on related systems.[11] The magnetic properties of *bare*, ferromagnetic in bulk, metal clusters appear to contrast strongly with the above observations. Measurements have been performed in which iron clusters made by pulsed-laser vaporization (see below) were passed through a Stern–Gerlach deflecting magnet.[12] Deflections were measurable up to Fe_3; for larger clusters it was only possible to follow on axis *depletions* because of low signal-to-noise and the increasingly large number of associated m_s substates (each of which is deflected differently). The observations suggest that all bare iron clusters studied (Fe_x, $x < 18$) are high spin and that total magnetic moment increases linearly with particle size, extrapolating to a value somewhat larger than ferromagnetic bulk.[13,14]

Strong "ligand" perturbations induce coverage-dependent reorientation of metal surfaces in bulk samples.[15] Similarly there are examples of restructuring in catalytically active metal particles (>20 Å), when exposed to a reactive environment. For example, octahedral platinum particles when exposed to H_2S are coated with a sulfide layer, which induces a restructuring to cubic habit.[16] Such experiments imply that, for strongly binding surface moieties, coverage effects may dominate cluster properties even to particle sizes, much in excess of the 100-atom limit set for this review.

Ligated metal clusters are therefore *not representative* of bare species in the size range treated here, precisely because of their coordinative saturation. For this reason, IR photodissociation experiments on transition-metal clusters complexed with IR-absorbing surface moieties [e.g., $Fe_x(CH_3OH)_y$[17]] are not likely to yield structural information on the precursor bare metal cluster unless coverage is kept to an absolute minimum.

In contrast IR photodissociation of *van der Waals complexes*, e.g. Fe_xAr, could prove feasible in this regard.[18] The following discussion will be confined to coordinatively unsaturated *bare* metal clusters.

1.3 Goals

(i) Phenomenological Theories of Metals and Alloys

The long-range goals of theoretical treatments in this field are quantitative prediction of structures (equilibrium and low-lying isomers) and (collective) electronic and thermodynamic properties and for multicomponent clusters composition and segregation effects, each as a function of cluster size. Furthermore and most importantly, this should be possible with one theory that extrapolates correctly to bulk lattice *and* molecular limits. At present, separate constructs describe the two extremes. These employ related concepts but often different and sometimes mutually exclusive terminology. It seems questionable whether either approach will ultimately fulfill the above specifications.

Bulk metal theories that typically rely on infinite lattice translational symmetry to simplify the problem (e.g. the HMO-related, nearly free electron model, etc.) break down when treating small particles with their associated structural anisotropy and finite boundaries. Artificial singularities may be generated when these theories are applied to systems with the same dimensions as the appropriate characteristic length.[19] Note that bulk theories also fail in describing amorphous and molten metals.

At the molecular limit, symmetry considerations provide much useful *qualitative* information. However, most semiempirical approaches making use of symmetry simplification have failed *quantitatively* for lack of accurate potentials. Descriptions of clusters on the basis of ab initio unrestricted Hartree–Fock calculations could provide these potentials and have been attempted for species with less than several tems of atoms (depending on the element[20]). The results, particularly for alkali clusters, are generally in good quantitative agreement with experiment. As bonding effects make up only a tiny fraction of the total energy, larger basis sets become necessary and computational involvement increases exponentially, with increasing cluster size. At present even the fastest computers run into time problems: one of the largest metal clusters yet calculated at an ab initio level is Be_{55}, which for one *predetermined* geometry requires 8 h of Cray 2 CPU time.[21] One is then faced with a pragmatic limit: the detailed theory should be applicable if carried to the extreme, but the answers may not be obtainable in an affordable calculation, at present technology. Furthermore and more importantly (considering the rapid development of computing power as a function of time),[22] physical insight anticorrelates with the size of the basis sets used and can only be retrieved—if at all—by comparing many calculations.

Clearly the alternative should—ultimately—*not* be a phenomenological theory providing some physical insight but little predictive power (e.g., jellium model). Experimental cluster science may serve a valuable role here by generating relevant particle specific data that act as a shortcut to the development of comprehensive *cluster* theories of metals and alloys.

(ii) Role of Clusters in Catalysis

The relevance of gas-phase bare metal cluster studies to heterogeneous (and homogeneous = microheterogeneous) catalysis is often stressed. In this context it has been proposed that there may be cluster sizes (or compositions in the case of bimetallics), which for a specific metal/support/reactant combination, are highly catalytically active due to their characteristic electronic (band gap, ionization potential, metal/non-metal transition, spin multiplicity), geometric (surface defect density, epitaxy effects), or temperature/phase properties.

In heterogeneous catalysis involving supported metal clusters, one traditionally differentiates between facile and demanding reactions[23] (also called structure sensitive and insensitive, respectively). Facile processes appear independent of cluster dimensions apart from the zero-order dispersion effect of surface to volume ratio. Demanding reactions manifest pronounced particle size dependence and motivate studies into the reactivity of bare species that generally stress steric rationalizations.[24] It is important to keep in mind that small clusters, even of refractory metals, have melting points well below the bulk as has been determined by electron microscopy.[25] Recently heterogeneous catalysts have been newly classified into those having equilibrated metal surfaces (EMS) and those with metastable metal surfaces (MMS).[26] EMS catalysts, which make up the bulk of, if not all, industrial catalysts (both for facile and demanding reactions), are characterized by operating temperatures close to the Huttig temperature ($T_m/3$). It appears that metal particles in the size range commonly used for industrial catalysis (20 Å) have sufficient surface mobility near this temperature that an "equilibrated state of several crystal faces is reached". One can speculate that lower operating temperatures are not desirable because a molten surface is less susceptible to poisoning. The implication is then that industrial catalysts are often molten under operating conditions. Consequently mainly variations in electronic structure will give rise to *particle size dependence* in these systems. In order to be relevant, gas-phase studies then require control over and a knowledge of cluster phase and internal temperature. While not yet addressed, this is a problem that can in principle be solved.

More troubling is the question of matrix effects. From gas-phase studies we infer that electronic and geometric structure changes with particle size are most dramatic for clusters having less than 10 atoms (see below). On a conventional oxide support or in a zeolite this size range corresponds to a regime in which metal–support interactions are likely to be extremely strong with a high proportion of cluster atoms involved (rafting and charge transfer). Therefore, any particle size effects occurring in this range in the gas-phase are likely to be absent or different in heterogeneous systems. In contrast, for larger clusters, gas-phase studies may provide important insight into the chemistry of supported aggregates.

The strength of support perturbations can be probed for by studying the chemistry of structurally well-defined, monodispersed, clusters on supports. These will have to be generated by deposition from a beam, as in situ generation has failed to provide satisfactory levels

of size and structural uniformity.[32,33] Even if the result of such measurements preclude homologies between condensed and gas-phase aggregates up to quite large particle sizes, it is conceivable that beam studies of small clusters may still lead to the development of novel gaseous catalytic or stoichiometric processes.

(iii) Cluster Materials

Rapid cooling ($>10^8$ K/s) of molten alloys leads to the formation of amorphous metals (metallic glasses) with neither positional nor orientational order.[34] These materials have interesting properties quite distinct from their crsytalline congeners (for example, high corrosion resistance). Under certain conditions and for specific metal combinations (Al–Mn, Al–Li–Cu, and several others), amorphous metals may contain regions with dimensions of up to 3 mm yielding electron diffraction patterns indicative of crystals with fivefold translational symmetry (icosahedral phase).[35] Space-filling fivefold symmetry is not possible for a crystalline lattice. Two explanations have been proposed: (a) a 3-dimensional Penrose tiling involving two different rhombohedric unit cells (quasicrystals); (b) a cluster material consisting of packed icosahedra (for example in Al–Mn: $Al_{12}Mn$) having the same overall orientation but joined randomly at edges and/or vertices.[35] The latter picture is supported by scanning tunneling microscope (STM) studies of glassy metal surfaces, showing evidence for clusters embedded in an amorphous matrix (of even smaller clusters?).[36] Note that cooling rates necessary for the production of quasi-crystals with relatively large dimensions appear to be lower than for metallic glasses.

There are many indications that microclusters have equilibrium structures that deviate dramatically from the crystalline bulk. Depending on cooling rates, cluster sources may generate these structures together with many slightly less stable valence isomers. In the case of bimetallic expansions, clusters with "impossible" stoichiometries can easily be formed. Given control over particle size distributions, it is conceivable that novel cluster materials may be formed by deposition of paucidispersed aggregates from a molecular beam.

2. Experimental Section

2.1. Sources

Gas-phase cluster studies are still limited by the sources available. The goal is to be able to routinely generate high-flux ($>10^{15}$ cm^{-2} s^{-1}), continuous, and monodispersed cluster beams with well-defined and selectable internal temperatures. Furthermore, there should be sufficient control over the expansion as to allow for (1) selection of a particular low-lying isomer and/or (2) generation of a well-defined equilibrium distribution of isomeric forms.

Sources for *monodispersed* clusters do not yet exist. Multi-metal organometallic complexes (or Zintl salts[37]) would appear to provide the ideal starting point for the generation of gas-phase (bare) transition-metal clusters of one size. However, low room-temperature vapor pressures and the low thermal dissociation thresholds associated with larger complexes make volatilization difficult. This problem can be circumvented if thermospray[38] or electrospray[39] techniques are used. A more serious shortcoming concerns lack of efficient methods for the stripping of ligands. Apart from some electron-impact studies,[194] most efforts in this area have involved one-color, visible or near-UV, pulsed multiphoton dissociation/ionization (MPD/MPI) of metal carbonyls. At high enough laser fluences one observes sequential absorption of up to 7 photons, leading to the formation of mainly atomic cations with small amounts of cluster ions.[41] While the exact mechanism is not known, efficient fragmentation of the central metal core must occur either during or subsequent to ligand stripping.[40] Later experiments using two-color visible irradiation with appropriately timed laser pulses and weakly bound ligands have achieved slightly higher cluster ion yields.[41] However, in general, this approach seems to be limited by a fundamental dissociation rate problem.

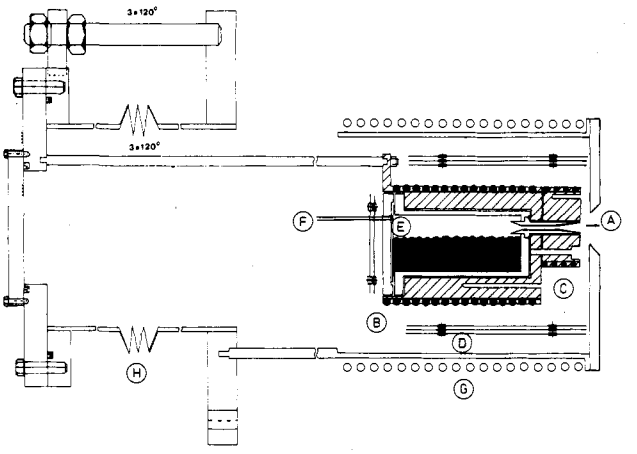

Figure 1. Schematic cross section of a high-temperature oven used to generate clusters of volatile metals by either neat vapor or seeded beam expansions. Metal samples contained in compression sealed or welded cartridges can be conductively heated (separate body and nozzle heaters) to temperatures of greater than 1300 K. To prevent clogging, nozzle temperature is usually kept 50 K higher than that of the cartridge body. Nozzle geometry used depends on the desired cluster size range and temperature distribution. Large alkali clusters (M_x, $x < 120$) can be conveniently generated by expansion out of 0.6-mm throat diameter, 30° (full angle) conical nozzles. Specifically identified in the diagram: conical nozzle, A; cartridge body and nozzle thermocoax heaters, B and C; tantalum radiation shields, D; chromium-plated copper sealing gasket, E; seed gas inlet, F; water-cooled heat shield, G; bellows for beam alignment, H. Details concerning experimental methods used in photoionization studies on supersonic beams of alkali clusters can be found in ref 42.

Size *distributions* of neutral and ionic gas-phase clusters can be produced for just about any metallic (and also nonmetallic) element in the periodic table. Methods used include continuous (high-temperature ovens; see Figure 1) and pulsed (laser vaporization) seeded and nonseeded supersonic expansions, incident-ion or metastable neutral beam sputtering of metallic targets, and gas aggregation of monomers generated either by thermal means or by cold cathode discharge. Most of these sources have been described at length in a recent review.[42] None provide good control over cluster phase, internal temperature, or size distributions. Measurement of these properties is itself not free of ambiguities. Applicability of individual cluster sources is a function of metal cohesive energies; for example, continuous expansions from high-temperature ovens are limited by materials considerations to the more volatile elements (a metal vapor pressure

of approximately 100 Torr is required).

There are dramatic differences with regard to the cluster fluxes available from different source configurations. Highest fluxes are obtained for continuous, neat, volatile metal vapor expansions out of high-temperature ovens, which can under favorable conditions provide at least 10^{15} cm^{-2} s^{-1} of one particular size (M_x, $x < 10$), 60 cm downstream from the source. Assuming 10% ionization efficiency, which is easily achievable for dimers,[43] and a collection and separation efficiency of 10%, this works out to monodispersed ion fluxes of 10^{13} s^{-1} (space charging problems can be solved[44]). Given a surface site of 100 Å^2, it would take 10 s to generate a monolayer by deposition, assuming a sticking coefficient of unity and negligible fragmentation upon beam–surface interaction.

At this writing the situation with regard to refractory metal clusters is less promising. Mass-separated, cluster cation fluxes, M_x^+ ($x < 10$), of up to 10^{-12} Å (6.43×10^6 particles s^{-1}) have been measured for an ion cluster beam generated via high repetition rate (500 Hz), pulsed laser vaporization under a continuous flow of carrier gas, followed by electron-impact ionization in the expansion zone.[45] Cold cathode discharge sources yield roughly 1 order of magnitude more mass separated cluster ion flux.[46] In both methods, neutral cluster fluxes are as yet not quantified but likely not more than 2 orders of magnitude larger. There have been claims of somewhat higher separated cluster ion currents using ion beam sputtering of metal targets (cold reflex discharge ion source for the primary beam that delivers several milliamperes of Ar^+ at 20 keV).[47]

2.2. Separation

In the absence of operative monodispersed neutral cluster sources, particle-specific studies require one or a series of separation stage(s) either prior to or during the measurement itself. Many methods have been proposed; several have at this writing been demonstrated. Among individual techniques, photodetachment of electrons from mass-selected negative cluster ions presently best meets throughput (low loss even though some fragmentation occurs) and separation efficiency requirements.[48] While not a separation scheme, coupling of a mass spectrometers to an ionization method that is cluster size sensitive (e.g., resonant two-photon ionization, R2PI) can provide size-specific information on the precursor neutrals if fragmentation and saturation effects are understood; see 2.4(i).

(i) Deflection

Constituents of a supersonic cluster beam, to first order, have uniform horizontal (on axis) but slightly mass-dependent vertical velocity distribution[42,63] (see below). Separation can be achieved by imparting large, cluster size dependent vertical velocity components. For example, clusters passed through an inhomogeneous magnetic or electric field experience deflection proportional to their respective magnetic or electric moments and inversely proportional to mass.

Attempts to magnetically deflect homonuclear alkali clusters have met with limited success,[49] due to strong spin–rotation coupling that increases in magnitude from Li to K and tends to average out magnetic moments.[50,51] For sodium, the effect precludes separation of Na_x ($x > 2$).[50,51] In contrast, spin–rotation coupling does not appear to be a problem for Al_x[52] or Fe_x[12] for which deflection has been reported. In such an experiment the magnitude of maximum deflection, d, from the beam center line as measured at the detector is given by eq 1, where μ is the cluster magnetic moment (averaged over all contributing states), dH/dz the gradient of the magnetic field, L the length of the magnet, m the cluster mass, D the distance from the end of the magnet to the detection region, and v the velocity of the species through the magnet. Unfortunately, in Fe_x, the magnetic moment appears to scale linearly with x such that deflections are size independent.

$$d = \mu(dH/dz)L^2(1 + 2D/L)/(2mv^2) \quad (1)$$

In an electric defelection study, sodium and potassium cluster beams were passed through an inhomogeneous transverse electric field. Deflections occurring are proportional to dipole moment times electric field gradient. Results obtained were interpreted purely in terms of induced moments, the mean static polarizability α being averaged over the "relevant molecular states".[53] Then, as induced dipole moment (αE) and field gradient are both proportional to the root-mean-squared static dipolar electric field E, deflections are given by eq 2, where L is the electrode path length, m the cluster mass, v its velocity, and K the apparatus function that includes flight path from deflecting field to detector. Per atom polarizability was found to be only weakly (and monotonically) dependent on cluster size (50% change between atom and bulk), such that separation of sodium and potassium clusters by electric deflection does not appear viable. In contrast, there have been some preliminary measurements on mixed-alkali species, in which separation according to permanent dipole moments was observed.[54]

$$z = K\alpha E^2/mv^2 \quad (2)$$

Photodeflection via resonant absorption and associated transfer of photon momentum has been demonstrated for beams of alkali atoms[55] and, using tunable cw-dye lasers, for atoms and dimers,[56] spontaneous emission being isotropic. It has yet to be applied to larger species due to two difficulties in addition to the mass problem: (i) The larger the cluster, the higher the density of states; consequently, for the same terminal temperatures, less population is available in one specific state for resonant absorption. (ii) Excited atoms can rapidly and efficiently reemit to the ground state, allowing for multiple excitations and incremental deflections during passage of the interaction region; in contrast, excited-state *molecules* can emit to many different states, most of which can no longer absorb; consequently the likelihood of multiple deflections is very low.

Momentum may also be transferred by scattering with a secondary beam. In studies of van der Waals and hydrogen-bonded aggregates, requiring rigorous particle specificity to sort out the details of ionization-induced fragmentation, measurable angular/velocity separations have been so achieved. In this experiment, a neutral cluster beam is crossed at right angles with a He beam.[57] Possible cluster trajectories are defined by a solid angle dependent on mass. For typical experimental configurations, attenuation levels upon crossed-jet scattering

of an argon cluster beam are about 10^6, with collision-induced dissociation only a significant problem for very weakly bound species. Such kinematic separation has also been attempted with sodium cluster beams.[58] Preliminary results suggest discontinuous size-dependent variations in scattering and collision-induced fragmentation cross sections. Free jet deceleration by countercurrent collision[59] has been applied to large clusters of copper and silver. The results are not unequivocal due to the lack of mass spectrometric characterization; however, they are consistent with significant particle size discrimination.

(ii) Mass Spectrometric Methods

An obvious route to monodispersed clusters is via generation of cluster ions (either by ionization of neutrals or by ion clustering), mass selection, and subsequent reneutralization–negative cluster ions by electron photodetachment[48] and positive ions by resonant or near-resonant collisional charge transfer.[60] Photodetachment has been demonstrated for several transition metals. Typically yields are quite high, but for certain metals, notably Ag and Cu, fragmentation to smaller cluster ions plus one or more neutral molecules is a strongly competitive process.[48] Fragmentation also appears to be a problem in collisional charge transfer. A recent study on sulfur cluster cations in which fragmentation is probed for by measuring the additional divergence of the resultant neutral beam (translational spectroscopy) concludes that the energy deficit of the charge-exchange process has to be kept as small as possible in order to minimize competing fragmentation.[61] There have as yet been no direct studies of resultant neutrals for either scheme. Clearly internal energy distributions are likely to be large and overall separation efficiencies low.

In the near future, generation of and deposition from monodispersed ion beams *without subsequent reneutralization* is likely to be a more viable approach to the deposition onto surfaces or into matrices of neutral clusters having very limited size distributions.[62]

(iii) Untried Methods

Two dynamic effects associated with supersonic expansions can be used in series to obtain partial size separation. (a) In seeded beams with large mass mismatches between heavy seed and light carrier gas, significant on-axis velocity slip of the heavier component occurs. An analogous effect is observed in seeded *cluster* beams:[63] velocity differentials of up to 20% have been found between the lightest and heaviest potassium clusters, K_x ($2 < x < 120$), generated by potassium in argon-seeded expansion.[64] On the basis of observations made in supersonic neat water vapor expansions,[65] cluster size dependent velocity differentials are also expected for pure metal vapor expansions. (b) Minor separation effects according to mass-dependent variations in perpendicular velocity distributions are also well-established. In cluster beams this leads to on-axis enrichment of heavier aggregates.[42]

A possible sequence of steps that would take advantage of beam dynamic mass separation to achieve a high degree of paucidispersion involves (a) rough control of cluster distribution by variation of stagnation conditions and nozzle geometry (dramatic enrichments of "magic" species may already be achievable here if expansion conditions are selected so as to favor the expression of relative thermodynamic stabilizies; see below), (b) high collimation and associated on-axis enrichment of heavier species, (c) inert-gas scattering to preferentially remove lighter species, (d) velocity selection, and (e) elimination of the largest clusters still present by near-threshold ionisation and extraction of ions. IP's generally decrease with cluster size, such that the larger clusters can be selectively ionized.

2.3. Detection

The most elementary questions occurring in gas-phase cluster studies concern the presence or absence of a beam and its composition. Several methods have been applied to the detection of metal species: (a) overall beam flux measured by deposition onto an oscillating quartz film thickness monitor;[66] (b) laser-induced fluorescence (LIF) measurements, providing some trimer data;[51,67,68] (c) electron diffraction;[101-103] (d) ionization of neutral species and detection of resulting ion currents, yielding by far the most information on metal clusters.

The most commonly utilized ionization modes in cluster studies are electron impact, thermoionization, and photoionization although Penning and collisional charge-transfer ionization have also been applied. Cluster parent and fragment ions have been measured as total currents with ionization gauges and surface ionization detectors. These tools are particle specific only for (i) very low cluster fluxes, (ii) efficient conversion of M_n to n times M^+, and (iii) situations when pulse counting is used.[64] Preferentially employed are mass filters (magnetic sector, time-of-flight, FTMS (Fourier transform ICR), Wien, quadrupole, ...) followed by determination of ion currents. Mass spectroscopic studies of metal cluster beams, particularly those directed toward determining neutral beam compositions, suffer from three effects that are generally poorly understood:

(i) Mass-Dependent Instrument Response

Often mass spectrometers are mounted perpendicular to the cluster beam to prevent detector contamination. It is clear that, due to the Thomson parabola effect,[69] cluster ions with roughly size-independent velocity and therefore linearly size-dependent kinetic energies will have different permissible ionization regions. Trajectory calculations for Na_x^+ ($x < 66$) moving through the ion source of a perpendicularly oriented quadrupole mass filter show that the volume mapped out by all accepted starting points is roughly conical, with the cone apex position and angle being a function of mass. Consequently and in particular for ionization methods with small interaction volumes—as is the case for focused laser irradiation—size-dependent ion source throughput is obtained, typically discriminating against heavier species.

Monotonic mass-dependent variations in filter transmission are also a common problem. For example, in a quadrupole filter, throughput is highly dependent on entrance aperture potential due to fringe fields from the rods.[70] In contrast, mass discrimination was thought to be negligible at quadrupole exit apertures because of the high detector potentials subsequently encoun-

tered by the ions. This assumption has been proved erroneous for heavy ions: the application of a 100-V positive potential to the exit aperture can result in an increase in ion detection efficiencies by up to a factor of 20 for $m/e > 500$.[70]

Once through the mass filter, ion currents are measured either directly with a Faraday cup or indirectly via a particle multiplier (e.g., channeltron, CuBe secondary electron multiplier, microchannel plates, Daly detectors). Conversion of ions into electrons in the first stage of such a multiplier is strongly mass dependent. There are two effects to be aware of:[71] (1) A velocity threshold of about 2×10^4 ms^{-1} for secondary electron emission; above this threshold multiplier response grows linearly with ion velocity, and therefore for monatomic ions at constant (multiplier) *potential*, detector response goes as $(m/e)^{-1/2}$. (2) For elemental cluster ions having constant incident velocities, detector response scales linearly with the number of monomer units. Then, under realistic experimental conditions of constant ion potential and for ion velocities above the secondary electron appearance threshold, detector response initially increases, goes through a maximum, and subsequently decreases with increasing cluster size.[71]

For typical multipliers, high mass response is limited by the maximum voltage applied between entrance dynode and signal anode (e.g., 2 kV for channeltrons). Note that a 10^4 m s^{-1} velocity threshold for secondary electron emission implies that an m/e 1800 cluster ion needs to see a first stage potential of at least 3 kV in order to be detected. Higher detection efficiency for large (positive) cluster ions can be achieved either by floating the entire multiplier at a high potential or by using a "conversion dynode" that is biased at a high negative potential (>4 kV) and inserted prior to the first multiplier stage. Note that spectacular detection efficiencies for alkali cluster ions have been achieved using a Daly detector to which is applied a negative potential in excess of 8 kV.[72]

(ii) Ionization and Fragmentation Cross Sections

Apart from instrument response, a detailed understanding of the ionization process itself is necessary to be able to determine a precursor neutral distribution from a mass spectrum. This requires information on ionization and fragmentation cross sections, in addition to a knowledge of ionization potentials and consequently that fraction of incident radiation giving rise to ions. In early studies neutral cluster abundances were determined from mass spectra (1:1 correspondence assumed) without any consideration being given to these factors.

At this writing, there are still no measurements of relative ionization cross sections for metal clusters. In the absence of such data one assumes that clusters are roughly spherical (see below) and that to first-order ionization cross section near the appearance threshold, where competing effects such as ionization-induced fragmentation are thought to be insignificant, goes as the geometric cross section ($\alpha n^{2/3}$).[73] Photoionization cross sections for sodium clusters (Na_x, $x < 21$) are presently being measured by ion depletion methods (see below).[74]

Ionization-induced fragmentation can be a significant problem to the determination of precursor neutral abundances, particularly with a broad-band ionization source providing excitation energy well above the adiabatic IP. Two examples from alkali cluster studies make this clear: (a) Mass spectra obtained upon electron-impact ionization (electron energy >10 eV) of a sodium cluster beam show only Na_x^+ ($x < 5$), while near-threshold photoionization of an otherwise identical expansion resolves cluster ions, $x < 17$.[75] (b) A recent photoionization study on Na_8 shows that significant fragmentation to Na_7^+ occurs[76] when radiation more than 0.5 eV in excess of the vertical ionization potential is used. It is possible to determine the wavelength dependence of the ratio of direct ionization to fragmentation cross sections by performing several measurements on beams having different neutral compositions. The extent to which sodium cluster mass spectra obtained by broad-band photoionization are contaminated by fragmentation contributions can so be quantified. Staying with this example, one finds that under certain expansion conditions up to 39% of the total Na_7^+ ion signal obtained upon irradiation with the full output of a 1-kW Xe/Hg arc lamp results from Na_8, while the measured Na_8^+ signal underrepresents the Na_8 present in the beam by 10%.

Note that fragmentation effects may not only depend on the excess energy (above the ionization potential) imparted to the system. For molecules with greatly different neutral and ionic ground-state equilbrium geometries such as hydrogen-bonded clusters and many types of van der Waals clusters, vertical ionization even *at threshold* will always lead to fragmentation. Fortunately metallic clusters (M_x, $x > 4$) typically have similar neutral and ionic ground-state equilibrium geometries, as calculations at many levels of sophistication imply.[77] Consequently, they will not fragment upon near-threshold ionization [exception: group 2a and 2b molecules prior to their non-metal/metal transition (see 4.5)].

2.4. Spectroscopy

All of the tools that have been applied to probing electronic and geometric structure parameters of transient intermediates and cold molecules in beams are applicable to small metal clusters also, with the restriction that many different molecules often with overlapping absorption features are present simultaneously. Ideally the method should ensure particle specificity. However, in spectral regions with poorly overlapping cluster signatures, nonspecific tools can be applied. For example, *van der Waals and hydrogen-bonded* aggregates have been studied using LIF, CARS[78] (coherent anti-Stokes Raman spectroscopy), FTIR (Fourier transform infrared) absorption,[79] laser aborption (mid-IR with bolometric detection,[80] far-IR,[81] visible intracavity), Raman,[82] photoelectron spectroscopy,[83] molecular beam electric resonance, and microwave spectroscopy of various forms.[84]

Excepting dimers, fewer techniques have been applied to spectroscopic studies of neutral gas-phase *metal* clusters: one-photon ionization, resonant two-photon ionization (R2PI), and multiphoton ionization, LIF, LIAF (laser-induced atomic fluorescence, from dissociation products[85]), and ion depletion. There have been several recent reports of photoelectron spectroscopy on mass-selected cluster anions.[46,86] With the exception

of LIF and LIAF all of these methods are particle specific.

(i) Rovibronic Studies (M_x, $x < 10$)

R2PI is the spectroscopic technique most extensively applied to the characterization of small metal clusters (Na_3, $LiNa_2$, Li_2Na, Cu_3; see 3.1). A brief discussion of the methods limitations is therefore in order. Electronic R2PI generates ions by two-step absorption. The first (exciting) photon is tuned to a transition between the neutral ground and an excited electronic state while the second (ionizing) photon surmounts the ionization threshold. The method can provide particle-specific, rotationally and vibrationally resolved absorption spectra containing mostly information on excited electronic states (and some ground-state data via hot bands), if the ionization step is sufficiently fast to ensure measurable ion yields. In clusters, intermediate-state lifetime is a particularly important consideration as population can rapidly decay via several different channels (predissociation, nonradiative relaxation, interconversion), with decay rates increasing with particle size.[87]

A dramatic example of the influence of competing processes on R2PI measurements is provided by a comparison of CW and pulsed studies on Na_3. Recently reported has been the observation, by one- and two-color pulsed laser R2PI, of four excited electronic states of this molecule significantly to the blue[88] of the two red bands ("A" and "B") found initially by R2PI with continuous-wave (CW) lasers.[89] These new states have resolvable vibrational features but much shorter lifetimes than A and B states and were therefore never observed in the CW laser studies, which had previously attempted to map out the same spectral region. Note that ionizing laser power levels in those CW R2PI measurements were at most 25 W (unfocused) compared to event powers of $>2 \times 10^6$ W (also unfocused) for a typical excimer pumped pulsed dye laser.

Attempts to obtain electronic R2PI spectra for larger alkali clusters have so far been unsuccessful. It has been proposed that this is a general problem, due (i) to rapid predissociation for all intermediate states above the first thermodynamically accessible dissociation threshold[90] and/or (ii) promotion of electrons from lower lying orbitals in competition with the ionization step.[91] These effects will clearly be minimized in studies of low-lying excited electronic states using high intensities and short pulses.

Upon breakdown of electronic R2PI due to excited-state lifetime effects, ion depletion spectroscopy becomes informative.[93] Ion signals generated by fixed-frequency one-photon absorption are measured as a function of the energy of a dissociating laser. Upon resonance, reductions in ion signal are observed. In contrast to R2PI this method looks at small changes in large signals and is therefore subject to greater noise problems. An ion depletion survey of predissociative excited electronic states in Na_x ($x < 41$) is presently being carried out in our laboratory. Initial measurements using excitation energies of 2.5 eV find extremely large but size-dependent dissociation yields (absorption cross section convoluted with the dissociation rate).[94] In this energy range, sequential monomer loss appears to be the preferred fragmentation mode.[95] In a more detailed depletion study on Na_4 using several different excitation frequencies, we have found evidence for a strongly predissociative excited electronic state between 2.4 and 2.6 eV.[94]

For metal clusters, electronic-state densities are characteristically high near the ground state. In conjunction with rotational and vibrationial structure, this causes rapid spectral congestion with increasing particle size ("vibronic soup"). This effect is best illustrated in terms of a recent ab initio calculation on Fe_2 that finds more than 60 excited electronic states within 0.139 eV of the $^7\Delta_u$ neutral ground state.[92] Assignment of a ground-state symmetry from electronic R2PI or ion depletion spectra is obviously impractical here. Level congestion is not quite as serious for small clusters of simple (as opposed to transition) metals and for molecules with high symmetry where the ground state can sometimes be significantly more stable than the first excited state.

(ii) Other Methods (M_x, $x < 10$)

Even is it were possible to obtain electronic spectra with well-resolved features, free of electronic-state congestion, the determination of ground-state equilibrium structures from an analysis of rovibronic bands very rapidly becomes prohibitively difficult (perhaps already for M_x, $x > 6$). Various infrared and microwave techniques may yield rovibrational data that are somewhat easier to interpret; however, they suffer from low cluster oscillator strengths in the corresponding spectral regions as well as from a lack of particle specificity. The latter problem may be soluble by way of IR/UV two-photon ionization.

Other techniques that hold promise for structure elucidation in the size range up to about 10 atoms include electrostatic multipole focusing to determine static dipole moments and magnetic resonance measurements (NMR[96] or ESR,[97] both of which have been demonstrated for particles on supports but not in beams). A novel approach recently applied to transition-metal clusters is IR photodissociation of weakly bound surface absorbates (see caveats in 1.2). Some limited bond energy information can also be obtained for small clusters using Knudsen cell mass spectrometric techniques;[98] however, the conclusions of such measurements are strongly dependent on electronic-state densities and cluster symmetries, both of which are typically unknown.

(iii) M_x, $x \geq 10$

Determination of structures beyond the M_{10} range requires different methodologies. The recent application of 200- and 400-keV HRTEM (high-resolution transmission electron microscopy) to the study of *supported* gold clusters[99] shows convincingly that it is possible to image clusters with radii smaller than 10 Å at almost atomic resolution. Surface tunneling microscopy (STM) can even achieve atomic resolution[100] and can also simultaneously distinguish elements; however, the time required to obtain a "picture" is long. Furthermore, there are difficulties with high surface mobility of clusters and STM probe contamination. In both measurements one runs into the problem of statistics (representative pictures). Microscopy techniques not directly applicable to the determination of gas-

phase equilbrium structures could however be used to obtain relevant data should it prove ossible to deposit narrow cluster size distributions in a nondestructive fashion onto inert atomically flat supports (for example, by free-jet deceleration).

Structures are also determinable from particle or photon scattering measurements in beams—ideally on monodispersed, monoisomeric, rigid, oriented, and cold clusters! However, even with these perfect conditions deconvolution of scattering data is not straightforward due to intrinsic problems associated with finite particle size. So far, electron diffraction[101-103] and now EXAFS (extended X-ray absorption fine structure)[104] methodologies have been sued for cluster beams with comparatively large cluster size and internal energy *distributions*. Determination of topologies from observed scattering profiles or absorption fine structure is not totally unambiguous under these conditions.

2.5. Chemical Reactivity

A large amount of data relevant to the chemical reactivity of neutral transition-metal clusters has over the past several years been amassed using flow tube reactors.[27,28] Clusters are generated by laser vaporization, and the resulting pulsed beam is subsequently mixed with a reagent stream. Reactant clusters and product species, usually having ionization potentials above 5 eV, are detected by one-photon or multiphoton ionization using an excimer laser (F_2, ArF, KrF, XeCl) and time-of-flight mass spectrometry. While selectivity is probed for by assigning products and reaction pathways, size-dependent variations in relative reaction rates are measured by quantifying growth of products and depletion of reactants (as ion signals). There have been several noteworthy conclusions from these experiments.[29-31] (1) High selectivities (even after taking dispersion into account, with enormous size-dependent variations in reaction rates are are seen for those reactions in which electron transfer is necessary to mediate the adsorption step (e.g., hydrogenation of Fe_x and Nb_x). Here rates, as measured by neutral cluster depletions, can be beautifully correlated with cluster ionization potentials. (2) Size effects *typically* observed in flow tube studies are much smaller and poorly resolved. Here definitive measurements and correlation with the details of electronic and/or geometric structure await the solution of a number of problems: (i) ionization potentials and cross sections for product species (and often reactant clusters) are typically poorly characterized; (ii) ionization-induced fragmentation is poorly understood; (iii) reaction pathway determination is ambiguous because the method is not strictly particle specific; (iv) there is no detailed knowledge or control of internal temperature; (v) it is not clearly established whether cluster growth is influenced by reagent addition; (vi) the magnitudes of scattering and collision-induced dissociation cross sections are unknown for reagent clusters.

The gas-phase chemical reactivity of main-group metal clusters has not been as extensively characterized. Apart from pulsed-flow tube measurements on Al_x ($x < 20$),[105] efforts have so far been limited to (i) supersonic beam studies of alkali cluster (Na_x, K_x, $x < 5$) oxidation by admixture of HCl, Cl_2, O_2, and N_2O to the expansion zone and analysis of products via photoionization;[106] (ii)

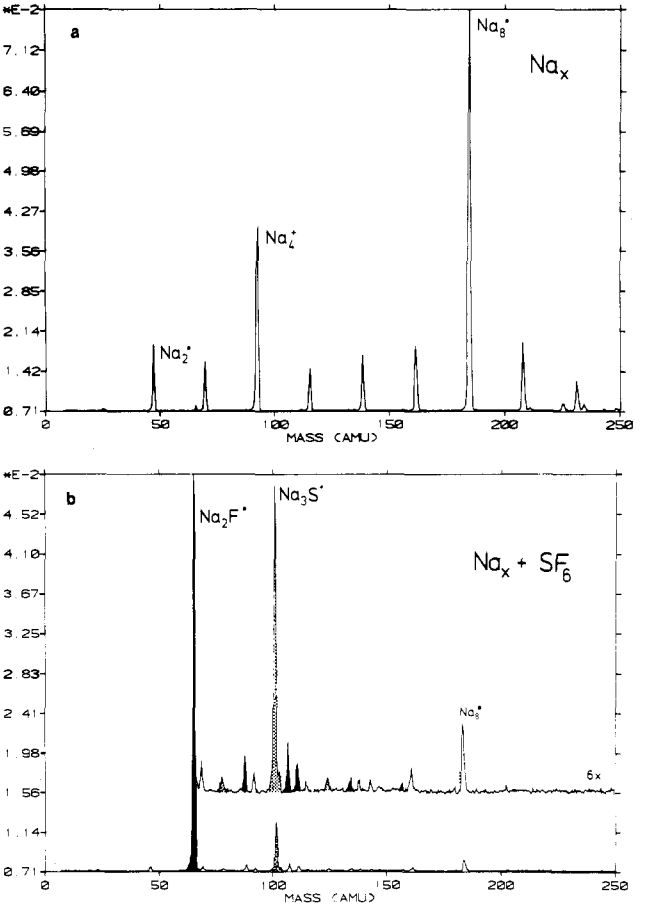

Figure 2. In a "pick-up" study, a sodium cluster beam was crossed with an SF_6 effusion, approximately 2 cm downstream from the nozzle. Shown are photoionization mass spectra (with the effusive beam off (a) and on (b)) obtained on the cluster beam axis by irradiating at 280 nm with use of a 1-kW arc lamp/monochromator combination. This corresponds to an energy sufficient to ionize all Na_x ($x > 2$) by absorption of one photon. Ion signals at $Na_xF_y^+$ (fully shaded) and Na_xS^+ (partially shaded) are indicative of neutral cluster reactions. Excepting Na_2F (see also ref 199), ionization potentials and ionization/fragmentation cross sections remain to be established for most products. Nevertheless, strong size-dependent variations in cluster reactivity are apparent.

characterization of size effects in reactions with chlorinated hydrocarbons, of Na_x and Zn_x ($x > 100 \pm 20$) generated by gas aggregation;[42,107] and (iii) "pick-up"[108] experiments on Na_x ($x < 41$) in which cluster beams are crossed at right angles with a reagent effusion (e.g., SF_6, O_2, N_2O, CCl_4; see Figure 2).[109]

In contrast to neutral metal clusters, the chemistry of cluster *ions* can be probed under rigorously particle specific conditions. Measurements have been performed mainly on positively charged species using (i) tandem or triple mass spectrometers[110-112] (with intermediate collision chamber), (ii) FTMS,[113-115] or (iii) SIFT (selected ion flow tube) techniques.[116] Initial results on positive cluster ions are fascinating but perhaps not quite as relevant to neutral cluster *chemistry* as hoped, for two reasons: (a) The influence of the positive charge is dominant up to at least M_{10}^+. (b) Internal excitation of cluster ions may be quite high and is at present poorly characterized and controlled. In contrast, some information pertaining to the *physical* properties of neutral species does result form these experiments: (i) Relative cluster ion stabilities obtained from photodissociation[87] and collision-induced fragmentation measurements[117] can be used to establish

neutral stabilities via ionization potential determinations. (ii) Ionization potentials may be bracketed by observation of charge-transfer reactions.[114]

3. Geometry

There is little experimental data relevant to the geometric structure of small metal clusters. Most of this information is from low-temperature matrix studies (e.g., absorption, Raman, Mössbauer, and ESR), which are not particle specific and often suffer from ill-defined guest–host interaction effects. Among main-group metals, matrix data are limited to Li_3,[118] Na_3,[119] and K_3,[120] all having Jahn–Teller distorted D_{3h} ground-state symmetries with small or nonexistent barriers to pseudorotation. There exists also an ESR spectrum tentatively assigned to a K_7[120] pentagonal bipyramid. Matrix measurements on transition-metal clusters[121,122] include Sc_3 (pseudorotating D_{3h} ground state, Y_3 (C_{2v}), Cr_3 (C_{2v}), Fe_3 (D_{3h}), Ni_3 (C_{2v}), Cu_3 (C_{2v}), Ag_3 (C_{2v}), Cu_2Ag (C_{2v}), Cu_5, Ag_5 (both distorted trigonal bipyramid), Cr_4 (tentatively assigned to a trigonally distorted tetrahedron, C_{3v}), Mn_5 (planar, pentagon), and Sc_{13} (ESR spectrum tentatively assigned to an icosahedral molecule).[122]

3.1. Trimers: Spectroscopic Data

There are only four gas-phase metal clusters for which there are vibrationally resolved spectroscopic data at this writing. These are all s-electron metal trimers: Na_3,[88,89,123] $LiNa_2$, Li_2Na,[124,125] and Cu_3.[67,93] While the ground state of Cu_3 (Jahn–Teller distorted D_{3h}) has been extensively studied by LIF,[67] most of the spectroscopic data for the other molecules have been obtained only via electronic R2PI and consequently contain very limited ground-state information. For none of the four s-electron trimers has a rotationally resolved spectrum yet been published. Therefore, ground-state geometries can only be assigned indirectly. In this context, study of Li_3, presently being pursued in several laboratories, is particularly promising because of the large rotational constants expected. *There are no other particle-specific gas-phase metal cluster data that allow inferences regarding ground-state equilibrium geometries.*

Of the four clusters for which we *do* have some information, Na_3 (Jahn–Teller distorted D_{3h} ground state) studies have been the most extensive. Experiments have mapped out all accessible visible absorption features, which encompass six excited electronic states in the wavelength range from 700 to 400 nm. Preliminary measurements suggest that excited-state lifetimes decrease with increasing energy.[123] The highest lying state yet studied cannot be observed in R2PI even with pulsed lasers (5-ns pulse width); instead it has been characterized by Na_3^+ ion depletion with simultaneous observation of the Na_2^* fragmentation product.[88] Detailed analysis of lifetime effects via picosecond probing would be useful here. R2PI measurements on Li_2Na and $LiNa_2$ have so far covered the spectral region from 700 to 520 nm. In each case, three electronic transitions quite analogous to those found for Na_3 have been recorded. Preliminary analysis of hot-band data and isotopic labeling experiments is consistent with C_{2v} ground states for both molecules.[124,125] Figure 3 shows the B system found for $^7LiNa_2$.

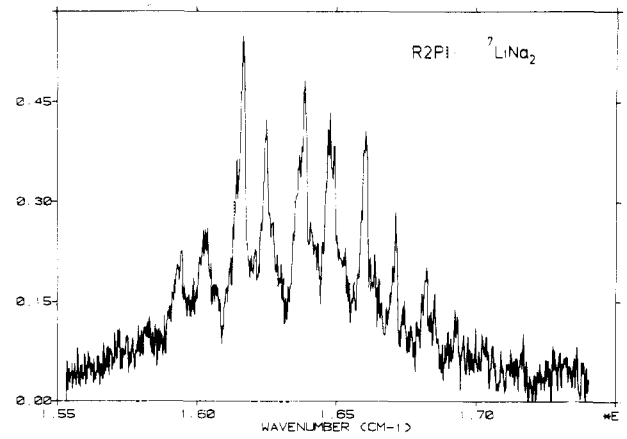

Figure 3. The visible absorption spectrum of $LiNa_2$ has been mapped out between 520 and 700 nm, using resonant two-photon ionization spectroscopy (1-W R6G CW dye exciting laser, 23-W CW Ar^+ green all lines ionization laser). Three excited electronic states, each with associated vibrational structure, have been identified and are found to correlate with analogous transitions of Na_3 and Li_2Na. Shown here is the "B" system consiting of a long vibrational progression in the excited (intermediate) state. R2PI with mass spectroscopic detection greatly facilitates isotope shift measurements ($^7LiNa_2$ versus $^6LiNa_2$), which in this particular case allow assignment of absolute vibrational number and inferences regarding geometric isomers (see ref 125).

3.2. Structure and Melting

The homonuclear trimers Na_3 and Cu_3 have nominal D_{3h} ground-state symmetries (^2E). As the HOMO is singly occupied, a Jahn–Teller distortion ensues, leading to three equivalent obtuse C_{2v} minima on the potential hypersurface. The molecule can interconvert back and forth between these minima by surmounting the acute C_{2v} saddle points, performing in so doing a large amplitude, fluxional motion called pseudorotation. The best way to think about this is in terms of an equilateral triangle for which each of the apical atoms undergo a correlated circular motion (120° out of respective phase) about the equilibrium positions. Depending on the barrier height, zero-point excitation may already suffice for pseudorotation. This appears to be the case for the ground state of Cu_3[67,126] but not for Na_3.[123] An interesting philosophical question ensues for Cu_3: how do we think of the equilibrium structure of a molecule that, according to the Lindemann criterion,[127] is molten in its ground state at the level of zero-point excitation. Obviously Cu_3 has time-average D_{3h} symmetry, but the most probable structure would appear to be a function of the probe duration. It is conceivable that fluxionality at the level of zero-point excitation is not just restricted to weakly bound trimers but can also occur as a consequence of Jahn–Teller distortion for larger, nominally highly symmetric clusters with partially occupied HOMO.

Clearly, metal clusters must generally be rigid at the level of zero-point excitation and only become fluxional when sufficiently internally excited. There is limited experimental information on melting in these systems, confined so far to particles larger than 10 Å. As mentioned above, cluster melting points have been shown to decrease with particle size.[25] According to molecular dynamics simulations on argon clusters, the concept of a melting *point* as a first-order phase transition loses

its meaning for small aggregates. It is replaced by two distinct temperatures: a freezing and a higher lying melting temperature.[128-130] The intermediate range comprises a coexistence region in which a specific cluster can exist for time periods long enough to exhibit equilibrium properties in one of the two forms before spontaneously interconverting (several nanoseconds). Coexistence regions have been observed in simulations for argon clusters with as few as seven atoms, and the implication is that they occur for smaller species also. Furthermore, the temperature width of the coexistence region appears to increase with decreasing particle size. Islands of enhanced relative thermodynamic stability lead to higher freezing and melting temperatures and narrower coexistence regions. There has, as yet, been no definite experimental confirmation of this concept.[131]

3.3. Isomers

For clusters that are not intrinsically fluxional and have internal temperatures within the rigid regime, it is conceivable that kinetically limited production methods involving rapid cooling such as laser vaporization generate an ensemble of isomeric forms that are probably not in thermodynamic equilibrium. In fact, it is conceivable that the *most* stable minimum on the potential energy hypersurface may not always be reached. While this has yet to be shown conclusively (perhaps by way of a hole-burning experiment), there are several beam experiments that can be so rationalized.[132] The facile production of glassy metals and quasi-metals suggests that this may be a serious problem to contend with when trying to determine a "representative" rigid metal cluster structure. Note that the determination of thermodynamic properties for metal clusters will ultimately require entropies and therefore a detailed knowledge of the structure and energetics of *all* accessible isomers.

The degree of isomer multiplicity can best be appreciated in terms of a simple example. Lennard–Jones pair potentials provide a first-order description of the bonding in van der Waals clusters. Several numerical search routines can be applied to finding the potential minima associated with a specific cluster size.[1] While it is not clear that *all* were in fact found, the count of distinct Lennard–Jones isomers obtained for A_n ($5 < n < 14$) is 2, 4, 8, 18, 57, 145, 366, and 988, respectively.[1] Clearly a different situation obtains for metal clusters; nevertheless, "isomer density" (number of distinct isomeric forms per unit excitation energy above the absolute minimum) is expected to increase *exponentially* with particle size.

3.4 Large Clusters

While beyond the scope of this review, it is pertinent to mention the structural information obtained for transition-metal clusers of several thousand atoms on supports—even though these measurements may suffer from epitaxy effects. Electron microscopy has shown microcrystallites with both bulk lattice habit and, particularly for very small species, pentagonal symmetry.[133] In such studies average interatomic spacings can be obtained from electron diffraction measurements on individual particles. These experiments provide firm evidence for lattice contraction (see Ionization Potentials and the Spherical Droplet Model), with decreasing particle size an effect understood macroscopically in terms of surface tension/surface free energy effects and microscopically in terms of optimized coordination and orbital overlap.[134] Note that EXAFS studies on supported clusters are in qualitative agreement with these conclusions.[135]

There have been several electron diffraction measurements on clusters in beams. Most extensively studied have been *van der Waals aggregates*. Two structural phase transitions have been inferred from measurements on various size distributions:[101] (i) Small clusters are thought to have multiply twinned icosahedral habit with a transition to multilayer icosahedral occurring at $n = 50$–80. (ii) Larger clusters assume lattice habit at $n = 800$–1000. Metal cluster electron diffraction studies can be similarly interpreted.[102] Here, structures commensurate with the bulk lattice habit seem to be thermodynamically favored at smaller particle sizes. It has not been established whether such structural phase transitions occur suddenly between M_n and M_{n+1}. However, there are intriguing reports of discontinuous variations in iron cluster chemisorption activity for NH_3 with particle size in the 60-atom size range.[136] Ab initio calculations are beginning to provide pertinent results. Total energies obtained for Be_{13} and Be_{55} clusters assuming high symmetry bulk (hcp) and fcc structures, respectively, show that the bulk structure is less stable for both sizes, while the total energy difference per atom between hcp and fcc forms has become significantly smaller at Be_{55}.[21]

4. Electronic Structure

4.1. Influence of Temperature

Clusters of s-electron metals have extensively delocalized, weakly directional bonding. Broad minima on the respective potential energy hypersurfaces lead to low thresholds for large-amplitude motion. Clearly, a knowledge of internal temperature is then of particular importance in correlating cluster ensemble geometric with electronic structure effects.

Cluster temperatures may be rigorously assigned on the basis of vibrationally and rotationally resolved (and assigned) spectra, *if* relative populations can be determined and a roughly Boltzmannian energy partitioning occurs. So far this has only proved possible for various metal dimers[137] and to a more limited extent for Na_3 and Cu_3. Typically for dimers formed by supersonic expansion a Boltzmann function adequately describes the vibrational and rotational state distributions encountered. Usually rotational and vibrational temperatures are *not* in equilibrium, with vibrational expansion cooling typically being less efficient. This is a function of metal and carrier gas by way of vibrational and rotational constants as well as interaction potentials. Dimer terminal temperatures depend on nozzle configuration and stagnation conditions. In neat sodium vapor expansions (350-Torr stagnation pressure) out of a 0.4-mm cylindrical nozzle at 1073 K one can achieve vibrational cooling down to ~50 K (T_{rot} = 35 K[43]), while the corresponding trimer number is ~100 K.[86] Seeded expansions can result in much colder clusters. R2PI measurements on Na_3 generated by seeding 10 Torr sodium into 8 atm argon yield trimer

internal temperatures closely approaching those of the dimer (T_{rot} = 7 K[123]).

At present, we have no quantitative data on internal temperatures of larger metal cluster species. During cluster growth large amounts of (binding) energy are released. This can only partly be removed by collisions, and therefore internal excitation is expected to increase with particle size. Clearly total energies above the respective first dissociation thresholds are rapidly reached, and *all* larger species become metastable. The largest cluster detected should be just cold enough to have survived the flight between source and detector without dissociating (further).[138] Rough limits on the temperature of mixed lithium/sodium clusters, generated in neat metal vapor expansions, have been assigned from studies of lithium enrichment relative to the vapor feed. These measurements imply that all clusters Li_xNa_y ($x + y > 10$) are molten upon leaving the expansion zone.[139] The question arises as to whether they are still molten at the detector.

Subsequent to expansion, the only possible cooling modes are radiative and evaporative.

(a) Radiative cooling of large clusters can be quantified from the Stefan–Boltzmann law reduced by the spectral absorption efficiency factor[140] (related to the ratio of spectral absorption cross section and actual cluster cross section), $E(\lambda)$ (eq 3), where ϵ_1 and ϵ_2 are

$$E(\lambda) = 12\pi D\lambda^{-1}[\epsilon_2[(\epsilon_1 + 2)^2 + \epsilon_2^2]^{-1}] \quad (3)$$

the real and imaginary parts of the cluster dielectric constant, D is the cluster diameter, and λ is the radiation wavelength). For a 1000-atom silver cluster at 1500 K one finds that the radiative energy lost during a typical 1-ms flight to the detector is more than a factor of 10 less than the heat of vaporization of a single atom. The situation is analogous for alkali clusters at somewhat lower temperatures and cohesive energies. Consequently significant radiative cooling before reaching the detection region is unlikely. Note that the same conclusion is reached if radiative lifetimes are considered.[141]

(b) A simple calculation shows that evaporation may be more important in reducing the temperature of nascent molten clusters: a 20-atom sodium cluster at 500 K has an internal energy of about 40 kcal/mol; consequently, evaporation of 1 atom at an energy of 20 kcal/mol is a thermodynamically if not kinetically accessible process.[139] Clearly, the development of particle-specific methods allowing for static and dynamic temperature determination in metal cluster beams is urgently needed. Possible routes include parametrization of ionization thresholds and measurement of fragmentation rates. In this context, the recent application of statistical mechanics to cluster fragmentation has led to the evaporative ensemble construct, which can be used to connect rates with internal temperatures directly.[138]

4.2. Ionization Potentials and the Spherical Droplet Model

A large part of the presently available data on the electronic structure of metal clusters comes from measurements of their ionization potentials and electron affinities. Ionization potentials have been determined for Li_x ($x < 5$),[142] Na_x ($x < 30$, x = 35, 40, 41, 45, 55, 60, 65),[143,144] K_x ($x < 101$),[143-145] Hg_x ($x < 13$),[146] Fe_x ($x < 25$),[147] Pb_x ($x < 8$),[148] Nb_x ($x < 29$),[14] V_x ($x < 23$),[14] Bi_x ($x < 39$),[149] Cu_x ($x < 30$; brackets),[150] and Al_x ($x < 26$),[117,152] while electron affinites are known for Cu_x^- ($x < 31$)[46,86] and Rb_x^- ($x < 4$).[152]. In contrast to metal dimers for which a rigorous determination of vertical and adiabatic ionization potentials has in several cases proved possible by way of spectroscopic analysis of autoionizing Rydberg series (both in R2PI and 1PI measurements),[153,154] assignment of cluster vertical ionization potentials is based on somewhat arbitrarily "deboltzmannizing" a slowly rising ion yield curve.[155] These curves, often obtained with highly structured radiation sources at finite dispersions for thermally excited clusters that either are molten or manifest broad isomer distributions, are typically featureless even at high resolution. Methods used for the assignment of *vertical* ionization potentials have ranged from linearization,[156] through Watanabe plots,[157] to step function computer fits.[76,144] Which of these methods yields the most accurate numbers depends on the resolution of the measurement and on (unknown) spectroscopic parameters of the molecular system studied. Various assignment methods have recently been contrasted in a publication containing measurements on Na_x ($x < 22$) at 2-nm resolution, using a spectrally flat radiation source.[158]

It has not yet proved possible to resolve autoionizing Rydberg features for any metallic cluster (see 4.5), let alone perform the spectroscopic analysis. In the absence of rigorous methods for the determination of *adiabatic* ionisation potentials, it becomes important to assess the influence of internal excitation on the numbers obtained. In clusters, it is likely that the average phonon energy at constant temperature is independent of particle size, as bulk Debye temperatures are often not greatly different from dimer vibrational constants. Then, if the probability of phonon-coupled ionization is not significantly size dependent, large contributions of internal excitation to appearance potentials[144] are not expected. For clusters at moderate temperatures ($T/T_{Debye} < 3$), internal excitation contributions should not exceed 5% of the vertical ionization potential. It is interesting to note that "phase-change" induced restructuring of electronic state densities may lead to changes in threshold laws.

Ionization potential data sets can be globally interpreted in terms of classical electrostatics.[159] Then, the numbers obtained represent the energy necessary to remove an electron from a uniformly conducting *sphere* having the same dimensions as the cluster. The difference between this energy and that needed to abstract an electron from a planar metal surface corresponds to a differential image force term plus a correction for the positive charge remaining at the center of the cluster cation. One obtains an expression connecting cluster ionization potential with bulk polycrystalline work function by a $1/R$ term, with clusters having high ionization potentials for smaller particle size. Recently there has been some controversy with regard to the correct slope of this term. A rigorous mathematical derivation puts it at $^3/_8e^2$ (eq 4), while an alternative

$$IP = WF + {}^3/_8(e^2/R) = WF + 5.4/R \text{ (eV; } R\text{, Å)} \quad (4)$$

more physical approach finds $^1/_2\, e^2$.[160] The data that

have been obtained thus far are all consistent with the former slope. For the determination of R one assumes $V_{cluster} = xV_{atom}$. Either the bulk atomic volume based on lattice constant or a number deriving from the dimer equilibrium bond length can be used. For simple metals, these are not greatly different (5%), and one can interpolate to obtain an intermediate cluster radius $R_x = r_x x^{1/3}$ (expressed in terms of the corresponding atomic radii) by making a surface tension correction that causes compression of small particles relative to bulk. Equation 5 results where κ and σ are macroscopic compressibility and surface tension, respectively, while r_∞ is the nearest-neighbor distance in infinite bulk.[161]

$$r_x = r_\infty \exp(-2\kappa\sigma/3r_x x^{1/3}) \qquad (5)$$

Agreement between data sets and classical droplet model is usually good, particularly for clusters with more than about 10 atoms. Figure 4a shows a representation of the presently available gas-phase metal cluster ionization potentials, in terms of a universal plot in which we present the difference in cluster ionization potentials and the corresponding bulk polycrystalline work function[162] predicted upon the basis of extrapolating the data to $1/R = 0$. Such extrapolations (which only make physical sense if a $^3/_8e^2$ slope is used!) come very close to accepted polycrystalline work functions for the simple metals. Significant differences between measured and extrapolated polycrystalline work functions are however observed for some of the transition metals and in particular Hg_x. Furthermore, small systematic deviations from the $^3/_8e^2$ slope become apparent in large data sets. This can still be rationalized classically in terms of variations in surface free energy as a result of dispersion.[163]

General agreement of spherical droplet predictions (slope and bulk extrapolation) with the ionization potential data has several implications: (1) The assumption of spherical symmetry is viable (metal clusters, M_x ($x > 10$), are not linear or planar!). (2) The size dependence of ionization potentials is overridingly determined by changes in curvature above the level of quantum size effects, which are typically not larger in magnitude than 10% of the IP. (3) Valence electrons are delocalized even for very small clusters. It is interesting to note that atom IP's extrapolate to within 25% of the bulk polycrystalline work function for most of the metallic elements of the periodic table.[162] Exceptions are groups 2a and 2b for which a nonmetal/metal transition has been postulated. Small molecules of these metals appear to be van der Waals clusters; see 4.5.

Quantum size effects lead to deviations of ionization potentials from the overall classical trend for small cluster sizes (M_x, $x < 10$). For example, M_3 and M_5 IP's for M = Na and K deviate strongly,[144] in each case because of a singly occupied nonbonding outermost orbital. Among larger alkali clusters, there have been reports of even–odd effects (see below) and for potassium clusters of minor discontinuities in ionization potentials that were correlated with the predictions of the jellium model of electronic structure (see 4.7).[144,145,156,158]

In general at least for the simple metals, ionization potential (and electron affinity) seems to be a property "swamped" by electrostatics and therefore not too sensitively dependent on the details of electronic or geometric structure *at presently achievable levels of cluster uniformity and low internal temperatures.*

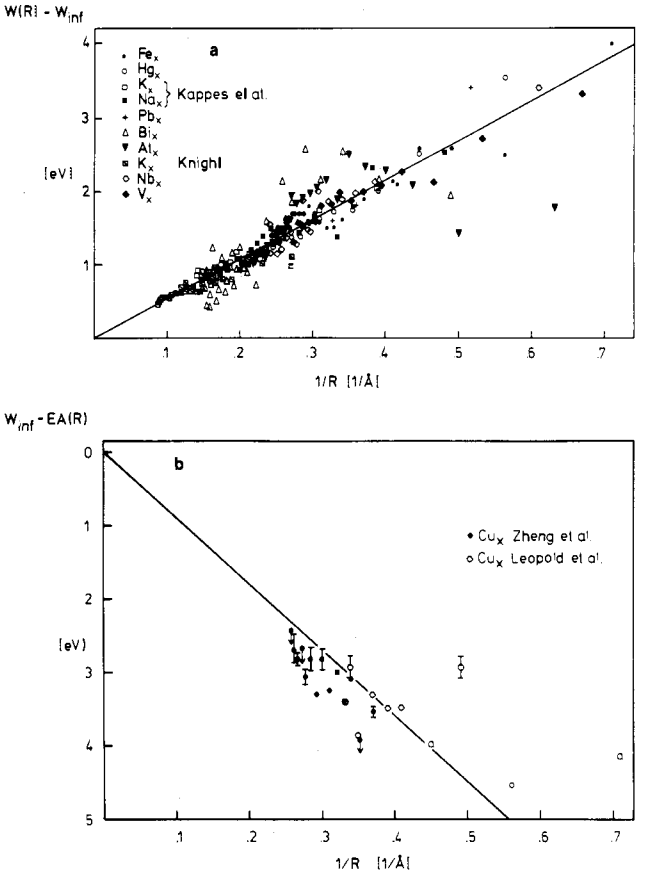

Figure 4. (a) "Universal" plot comparing all presently available metal cluster ionization potential data sets with the predictions of the classical spherical droplet model (eq 5). The difference between ionization potential and extrapolated work function, versus R, the radius of a sphere with the same volume as an x atomic metal cluster (assuming for consistency atomic volume derived from bulk density; $R_{cluster} = r_{bulk}x^{1/3}$) is plotted. Error bars for the respective measurements are not shown so as to enhance clarity; they can be found in the original publications (see 4.2). Largest error bars and also largest scatter from the droplet model pertain to the bismuth and aluminum data sets. In general, agreement with the model is good beyond M_{10}, with quantum size effects apparent at smaller particle size. Comparison of bulk extrapolations to experimentally determined polycrystalline work functions is typically reasonable [within 0.2 (Na), 0.07 (K), 0.25 (Pb), 0.67 (Fe), 0.84 (Nb), 0.94 (V), −1.10 (Bi), and 0.06 eV (Al)], except for Hg_x (−2.44 eV). (b) Analogous plot of the difference between copper cluster electron affinities and extrapolated work function according to eq 6, versus $1/R$ (Cu_x EA values are from ref 46 and 86).

4.3. Electron Affinities and Band Gaps

The energy released upon adding an electron to bulk metal is the same as required to remove an electron. For clusters, electron affinities can also be modeled in terms of classical electrostatics. One uses the same picture as for ionization potential without the correction for a residual positive charge.[46] Then an expression is obtained relating electron affinity to the work function again by a $1/R$ term but now with a different slope (eq 6); cluster electron affinities increase with increasing

$$EA = WF - {}^5/_8(e^2/R) = WF - 9/R \text{ (eV)} \qquad (6)$$

particle size. Recent experimental determinations of Cu_x^- electron affinities find roughly the expected

functional dependence on particle size above Cu_8 (see Figure 4b); however, extrapolation to the bulk work function is poor if the bulk interatomic separation is assumed[46] and becomes worse if surface tension and resultant cluster *compression* with decreasing neutral particle size is taken into account. It has been proposed that the additional electron associated with negative copper clusters *increases* the effective volume. Using such an additive correction to cluster radius then yields a much improved extrapolation.[46]

Note that Cu_x^- electron affinities obtained with a discharge cluster source likely reflect electron binding in molten clusters.[46] In contrast, studies of Cu_x^- produced by pulsed-laser vaporization are more likely to have probed an ensemble of rigid isomers.[86,164] Comparison of the two data sets is inconclusive in this regard, because of limited overlap in the cluster size ranges studied. Note that in bulk samples different single crystal faces can have significantly disparate work functions.[162] While, for very small particles, one cannot consider photoemission to be localized to one specific face, there will be opportunity to observe structural phase transitions in larger clusters ($n > 10^4$) via associated changes in electron affinities and ionization potentials.

Photodetachment cross sections postthreshold have also been recorded for copper cluster anions (Cu_x^-, $x < 15$).[46,164] Particularly for even clusters these spectra contain features identified with transitions of the ground-state anion to the first spectrally accessible excited state of the neutral cluster, thus providing information relevant to the HOMO–LUMO "bandgap" in *neutral* clusters. Inferences drawn from the data include that the bandgap for Cu_4 is 0.8 eV, already quite far into the IR, and that it decreases further with increasing cluster size. The gap varies roughly as $1/n^{1.8}$ over the limited size range studied, in contrast to predicted functional dependencies of $n^{-1/3}$ [165] and n^{-1} [166] for somewhat larger clusters. Interestingly for both data sets there is a pronounced discontinuity both in the size-dependent development of electron affinity and band gap, at Cu_8.

4.4. Multiplicities and Even–Odd Effects

There are several experimental observations obtained for clusters of s-electron metals, classified as even–odd effects.

(i) In ionization potential measurements on alkalis (Na_x, $x < 20$; K_x, $x < 20$) even clusters systematically have slightly (0.1–0.2 eV) higher values than their odd neighbors.[144,145,156,158]

(ii) Sodium cluster photoionization efficiency curves manifest an even–odd dependence of postthreshold ion yield (>0.5 eV) above the vertical IP), which can be explained in terms of lower ionization-induced fragmentation rates for odd clusters ions. This effect is observable up to an including Na_{41}^+.[167] Figure 5a–d shows PIE curves obtained for Na_{14}–Na_{21}.

(iii) An inverse effect is found for copper cluster electron affinity measurements, with odd clusters having higher photodetachment thresholds.[46,86]

All observations can be explained in terms of stabilization due to electron pairing and are consistent with neutral and ionic ground states having low multiplicities, in contrast to clusters of ferromagnetic metals such

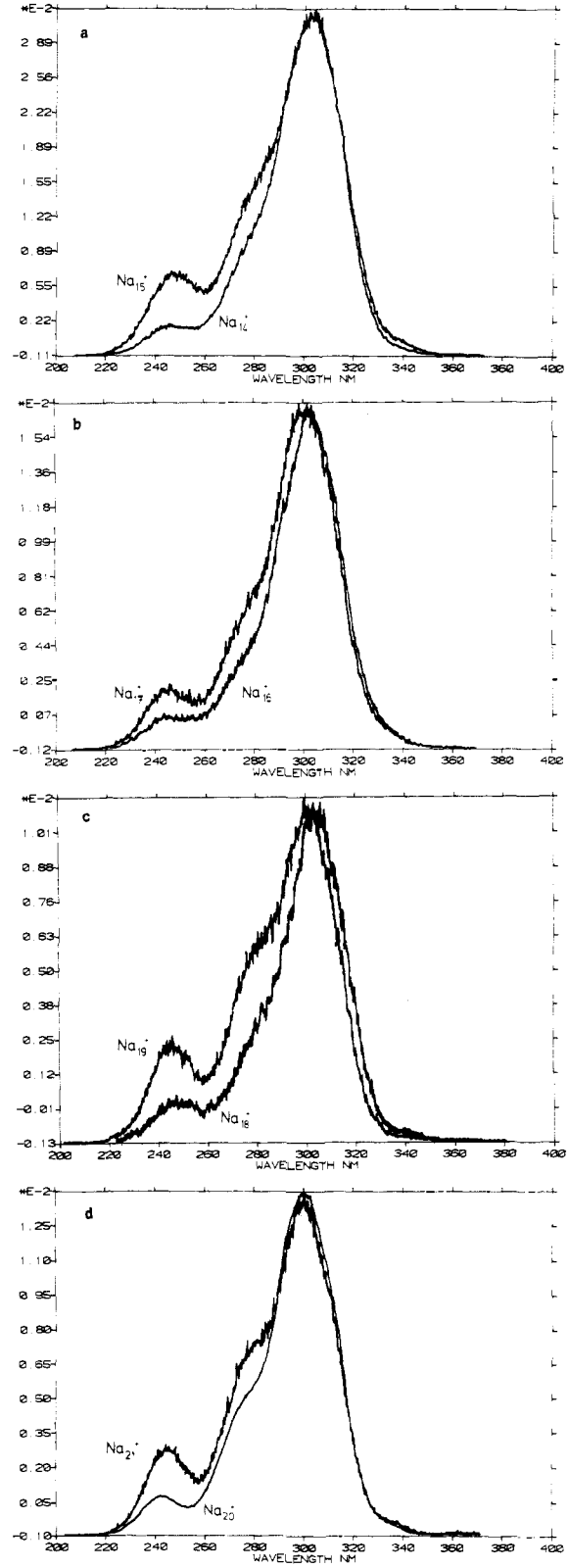

Figure 5. (a–d) Photoionization efficiency curves obtained at 20-nm resolution for Na_x ($14 < x < 21$). Most of the structure in these curves, which were not intensity normalized, results from the Xe/Hg lamp spectrum. However, there is a systematic even–odd effect in postthreshold ion signal (near 240 nm). These fluctuations, too large to be rationalized in terms of changes in ionization potentials, are due to variations in postthreshold fragmentation rate. The implication is that even cluster ions are slightly less stable than their odd neighbors (see 4.4). We have recently obtained high-resolution (2-nm) PIE curves for Na_x ($2 < x < 23$) using a Xe lamp that has an unstructured emission spectrum. In these measurements, even–odd effects are also apparent in ionization thresholds (see ref 158).

as iron, for which high magnetic moments are inferred; see 1.2.[168]

4.5. Core Levels and the Metal–Non-Metal Transition

One-photon ionization measurements on neutral clusters can provide information on lower lying occupied orbitals, if the radiation used is sufficiently energetic. The position of core orbitals is relevant to understanding the development of band structure and metallic properties with particle size. Strictly, the attribute metallic loses its meaning for small clusters. By operating definition a cluster becomes metallic, if (i) valence electrons are fully delocalized and (ii) there is a high density of unoccupied excited electronic states close enough to the HOMO such that their thermal population occurs.[144]

For an s-electron metal, development of band structure as cluster size increases is associated with an increasing number of s-correlating levels, half of which are occupied. Density of states increases exponentially, while the position of the highest occupied level relative to vacuum rapidly becomes insensitive to changes in cluster size (apart from curvature effects). As borne out by ionization potential and electron affinity measurements, clusters quickly become metallic according to the above definition (below M_7, depending on temperature), while cohesive energies tend monotonically toward bulk values with only minor particle size dependent fluctuations.

More complicated metals, with partially occupied atomic p and d orbitals, are thought to approach bulk electronic properties more slowly and discontinuously because of strongly directional bonding requirements. However, metallic behavior is still expected to set in below M_{10}, consistent with ionization potential measurements for clusters of various elements. For example after initially increasing with cluster size, Al_x[117,151] ionization potentials appear to conform to the classical functional dependence at $x > 10$ and extrapolate to within 0.1 eV of the experimentally determined bulk polycrystalline work function.

Clusters composed of group 2a and 2b metals show very different size-dependent changes in electronic structure. Atoms with fully occupied s-valence shells clearly give rise to clusters with fully occupied, weakly bonding, s bands. In such molecules, bulklike, metallic cohesion can only be achieved via overlap with a higher lying empty band. The closest is associated with unoccupied atomic p orbitals. The energy gap between s- and p-correlating bands will decrease with increasing particle size, as the corresponding band widths increase. Eventually a particle size is reached at which overlap occurs, resulting in measurable changes in electronic structure and perhaps a sudden increase in cohesive energy. The position at which s–p overlap occurs is not known; however, several recent experiments on mercury clusters provide some relevant data.[169] Note that groups 2a and 2b dimers are weakly bound van der Waals molecules.

Mercury clusters have extremely high ionization potentials, which can only be reached (tunably) with synchrotron radiation. Postthreshold photoionization efficiency measurements on Hg_x ($x < 9$) uniformly show two well-defined autoionization features that can be rationalized in terms of transitions from the center of a narrow 5d-derived band to the center of a 6p-derived empty band. Transition energies and doublet separtions change monotonically with increasing cluster size. As the doublet remains spectrally well-defined up to and including Hg_8, there is no indication of s–p band mixing throughout this size range. In this regard preliminary analysis of new measurements for Hg_x ($x < 40$) suggests that band mixing may occur below Hg_{20}.[170] Note that, in extrapolations to bulk of mercury cluster ionization potentials, there is a discrepancy between predicted and experimentally determined polycrystalline work function of 2.4 eV. Conceivably this is due to a sudden change in the position of the highest occupied molecular orbital upon s–p "band" overlap. Similar phenomena should also be observable for magnesium clusters that have the dual virtues of lower mass and lower ionization potentials for cluster sizes both above and below the purported metal/non-metal transition. From eq 4, the ionization potential of a *metallic* Mg_{40} is predicted to be 4.42 eV, an energy range conveniently accessible with tunable lasers.

4.6 Islands of Enhanced Thermodynamic Stability

(i) Quasi-Equilibrium

In metal cluster studies, "magic" numbers are often encountered in mass spectra. If appropriate precautions are taken to rule out artifacts and corrections made for ionization and ion fragmentation cross sections, it is ultimately possible to link these mass spectra to precursor neutral-intensity distributions.[171] In some cases, particularly for alkalis, "magic" numbers remain after correction, corresponding to particularly abundant neutrals. This behavior is generally restricted to source configurations that ensure high initial cluster temperatures with relatively low subsequent cooling rates. In contrast, kinetically limited cluster sources having high cooling rates, such as pulsed-laser vaporization, generally produce monotonically varying size distributions.[172] Note that it should prove possible to induce thermodynamically predicated discontinuities in neutral cluster distributions resulting from kinetically limited sources, by slowing the expansion or heating the expansion zone (e.g., via IR irradiation).

It is often assumed that dominant neutral clusters correspond to molecules with high relative thermodynamic stability. In reality, neutral cluster distributions are strongly dependent on expansion conditions, usually an almost *intractable composite* of thermodynamic and kinetic contributions. Stability inferences require an in depth understanding of cluster growth processes as recent studies on sodium and mixed sodium/lithium expansions have shown.[76,139] It is clear that a supersonic expansion can never quite reach thermodynamic equilibrium. However, the more collisions possible in the expansion zone, the more the resulting cluster distribution changes from kinetically to thermodynamically determined. For *high collision number* expansions of sodium and lithium metal vapor, binomial mixed-cluster distributions are observed in which lithium is enriched relative to the atomic vapor feed (Figure 6).[139] This enrichment is thermodynamically driven, and its extent is consistent with the attainment of

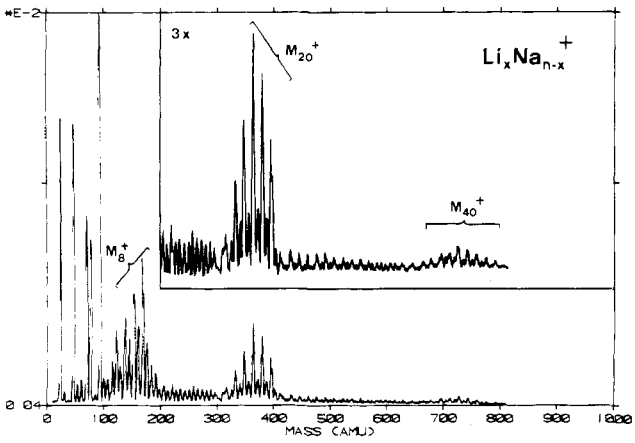

Figure 6. Photoionization mass spectrum obtained for a mixed lithium/sodium metal vapor expansion (T_{oven} = 1038 K, 0.6-nm 15° conical nozzle, 280-nm irradiation). Among cluster ions ($Li_xNa_{n-n}^+$, $n < 43$) having the same total number of atoms, roughly binomial distributions are observed. In these, the lithium statistical weights are a function of cluster size and in all cases greater than expected on the basis of lithium content in the atomic vapor feed (up to 40x). Lithium enrichment is thermodynamically driven, and its extent provides an indication that, for beams resulting from high collision number expansions, relative thermodynamic stabilities can be partially expressed in terms of neutral abundances.

quasi-equilibrium (if one makes reasonable assumptions concerning associated free energy changes on the basis of ab initio calculations for homonuclear alkali clusters).[77,186] Consequently, dramatically multimodal neutral cluster distributions resulting from equally stringent (and "nucleating") *homonuclear* alkali vapor expansions must also reflect differences in relative thermodynamic stabilities of the species involved.

(ii) "Magic Numbers": Alkalis

The first experimental indication of stability islands among neutral alkali clusters was obtained in a photoionization study on sodium clusters generated by a Campargue type, continuous seeded beam expansion[69] with seed gas to sodium pressure ratios of typically 5:1. The mass spectra obtained in that study showed broadly multimodal ion distributions with maxima observed centered at $Na_{7/8}^+$, Na_{19}^+, and Na_{38}^+ (and perhaps near Na_{55}^+) and local minima apparent at Na_9^+, Na_{21}^+, and Na_{42}^+. While relative heights of ion abundance maxima could be shifted by varying the carrier gas and associated degree of expansion cooling (He, Ne, Ar, Kr, N_2), their absolute position proved to be intrinsic.

In a subsequent seeded beam measurement,[72] mass spectra with much narrower and more pronounced ion abundance maxima (Na_8^+, Na_{20}^+, Na_{40}^+, Na_{58}^+, Na_{92}^+) were reported. This study utilized a different source configuration (Fenn type) with smaller nozzle aperture, higher seed gas to sodium pressure ratios, and expansion into relatively high vacuum ($<10^{-4}$ Torr). There has been some controversy and misunderstanding with regard to the differences between mass spectra obtained in the two experiments.[72,183] It has been suggested that the early measurement was flawed due to effects arising from differences in experimental arrangement used: (i) mass discrimination associated with perpendicular detector orientation and (ii) higher cluster temperature.[173] As subsequent experiments have shown, the first claim is invalid while the second is questionable in the absence of conclusive temperature determinations.[174] The role of collision-induced dissociation and IR photodissociation are presently being investigated in this context.[158]

Since the sodium-seeded beam measurements, there have been several other relevant experiments: (1) The same series of dominant magic numbers with slightly less pronounced maxima were observed for a Fenn-type seeded beam for K_x[175] and NaK_x ($x + 1$). (2) Independently neat metal vapor expansions through large aperture conical nozzles yielded identical potassium cluster mass spectra[144] and the same series of abundance maxima for Li_x ($x < 22$),[176] LiK_x ($x + 1$),[188] and Li_xNa_y ($x + y$),[139] respectively. Note that a later detailed analysis of ionization potentials and relative cross sections indicates that the tetramer is also quite abundant relative to M_3 and M_5 in *all* alkali expansions (see Figure 7).[176]

4.7. Bonding Models

Dominant ion "magic numbers" observed in alkali mass spectra have been explained in terms of a simple quantum mechanical model that attributes enhanced relative thermodynamic stability to neutral precursors.[72,187] In this model a uniform positively charged spherical potential well is assumed into which valence electrons—one electron per alkali—are filled.[177] Equation 7 gives the Woods–Saxon rounded-corner

$$U(r) = -U_0(\exp([r - r_0]/\epsilon) + 1)^{-1} \qquad (7)$$

finite square-well potential used in the first publication.[72] U_0 is the sum of Fermi energy and work function in bulk, r_0 is the effective radius of the cluster sphere (proportional to $N^{-1/3}$), and ϵ is a parameter that quantifies the variation of the potential at the edge of the sphere. Solution of the quantum mechanics of this problem is quite simple and results in a series of degenerate energy levels, the filling order of which yields a set of numbers that partially overlaps the series of dominant maxima observed in experiment. The cluster shell model is identical with the nuclear shell model, except for the neglect of spin/orbital angular momentum coupling effects not observed in alkali clusters.[178] Connection between closed-shell clusters and enhanced thermodynamic stability is made by way of the second difference in cluster energy as determined by the jellium model, which shows local maxima at closed-shell clusters. Figure 7b(i) compares these second differences to a typical sodium cluster photoionization mass spectrum obtained by expansion of neat sodium vapor (Figure 7a). Note that the degeneracy of levels, the order of their filling, and therefore the set of numbers generated depend somewhat on the well shape assumed: three-dimensional harmonic oscillator or infinite square-well potentials lead to slightly different numerologies.[179] Alkali photoionization mass spectra exhibit reproducible fine structure below the level of dominant ion abundance maxima. There has been a recent attempt at rationalization in terms of geometric perturbations of open-shell clusters.[180] As in analogous calculations on atomic nuclei, clusters are distorted ellipsoidally at constant volume and energy is minimized against distortion parameter that is a function of the major and the minor axes of the ellipsoid. Correlation of the

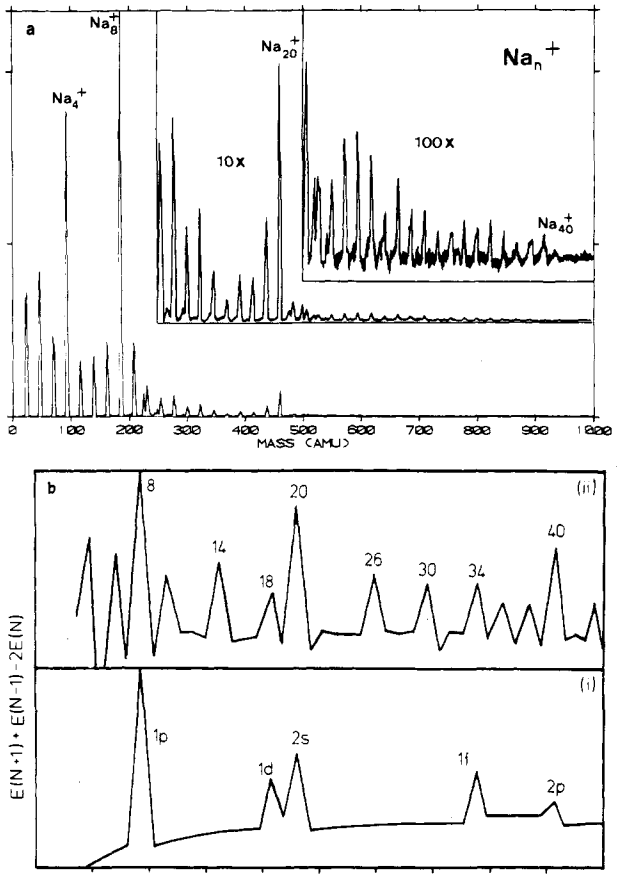

Figure 7. (a) Photoemission mass spectrum obtained for a sodium cluster beam (30° conical nozzle, 0.6-mm-diameter throat, T_{oven} = 1073 K). Clusters were ionized with 280-nm radiation, conditions minimizing ionization-induced fragmentation. The mass spectrum contains ion abundance maxima at Na_x^+ (x = 4, 8, 20, 40), corresponding to dominant neutral clusters at these masses (kinetic, fragmentation, and ionization cross-section influences can be ruled out; see 2.3). Identical mass spectra have also been obtained for sodium in argon-seeded expansions.[72] A jellium shell model has been recast to explain dominant neutral clusters in terms of islands of enhanced thermodynamic stability, associated with specific "magic" numbers of valence electrons. Connection between experiment and model is made via the second difference in jellium energy $[E(N-1) + E(N+1) - 2E(N)]$, plotted as a function of cluster size (N) in (b)–(i). Note that the nomenclature used in describing filled levels, (n, l), deviates from the spherically symmetric coulomb field problem where the main quantum number n' corresponds to $n + 1$. Recently this approach has been extended to include ellipsoidal distortions of the uniform jellium.[180] The results are shown in (b)–(ii). Both approaches are subject to some contention (see 4.7).

measurements with predicted fine structure in neutral cluster abundances is reasonable (see figure 7b(ii)); unfortunately, the details of these mass spectra are probably significantly marred by fragmentation effects.[76]

First restricted to alkalis, the jellium model has since been applied to the rationalization of ion abundance distributions observed for several more complicated s-electron metals: Cu, Ag, and Au.[181] All of these measurements directly probe ion stabilities; consequently "magic" (atom) numbers should be shifted up or down by 1, depending on whether positive or negative cluster ions are being studied. This is in fact observed. With few exceptions, group 1b cluster ions are produced by sputtering, a process that imparts much internal energy into the nascent molecules. *No studies* of s-electron metal clusters showing "shell structure" have been performed under conditions assuring *low temperatures and cluster rigidity*. Less successful attempts have been made to apply jellium calculations to metallic elements for which bonding is highly directional and for which electronic structure is strongly coordination and compression dependent (Al[117,182] and Pb[183]). Collision-induced dissociation studies on Al_x^+ ($x < 26$), which find evidence for a (geometric?) stability maximum at Al_{13}^+,[117] and ab initio calculations on Al_x ($x < 7$) are informative in this regard.[184]

The validity of the jellium approach has been subject to some contention[144,158,185] due to incomplete correspondence of model predictions with experimentally determined dynamic response properties such as neutral abundances, ionization potentials,[144] and polarizabilities.[53,179] Subsequent spheroidal distortion approaches have partially redressed this problem,[180] but the model still seems coarse in comparison to state of the art ab initio calculations that are able to describe stability maxima and dynamic response properties adequately for clusters with less than 21 atoms (present upper size limit of clusters calculated) *without* having to neglect molecular structure.[77] Albeit vibrationless geometries are obtained that are often far from spherical (planar up to and including M_6).[186] A pragmatic philosophy would uphold the use of jellium calculations for large s-electron clusters—there is nothing better available. A recent semiempirical treatment draws some insightful parralels between the two opposing approaches as applied to small clusters.[198]

4.8. Heteroatom Probing: Relationship between Electronic and Geometric Structure

Spherical shell models assume negligible contribution of geometric structure to total energy. When the jellium model was first introduced, it was proposed that the alkali clusters to which it was being applied were in fact rigid. This dichotomy led to the formulation of "heteroatom probing" experiments designed to gauge the relative magnitudes of electronic and geometric contributions to total energy: here alkali atoms are replaced by heteroatoms with more than one valence electron (and different atomic radius).[188] Then for a heterocluster M_xN with heteroatom valence electrons fully involved in (delocalized) metallic bonding, "magic" islands of enhanced thermodynamic stability, determined purely by the number of valence electrons, should be shifted by an amount appropriate to the total valence electron count. For example, if a potassium atom is replaced by a magnesium atom, which has two valence electrons, the model predicts a thermodynamically favored eight-electron jellium shell closing to be manifested as a neutral cluster abundance maximum at K_6Mg. Instead we observe an abundance and consequently stability maximum at K_8Mg. This can still be explained within the jellium model by invoking a centrally located heteroatom and a reversal in the filling order due to added stabilization of s-like cluster states with low angular momentum. However, ionization potential measurements on the series K_xMg ($5 < x < 10$) are harder to rationalize.[188]

Table I provides a summary of all hetereoatoms probing experiments performed to date.[189,190] Also listed are the ion abundance maxima observed (>5× intensity changes between M_nN^+ and $M_{n+1}N^+$ consitute a max-

TABLE I. Ion Abundance Maxima in Heteroatom-Probing Experiments

metals (M, N)	maxima (M_nN^+) n	valence electron counts[a]
Na/Li	7, 19, 39	8, 20, 40
K/Li	7, 19	8, 20
Na/Mg[b]	6–8, 18	8–10, 20
Na/Ca	6, 18	8, 20
Na/Sr	6, 16–18, 38	8, 18–20, 40
Na/Ba	6, 16	8, 18
Na/Zn	8, 18	10, 20
Na/Eu	6, 16	8, 18
Na/Yb	6, 18, 38	8, 20, 40
K/Mg	8, 18	10, 20
K/Zn	8, 18	10, 20
K/Hg	8, 19	10, 21

[a] Electron counts for precursor neutral clusters, assuming minimal fragmentation effects (see the text). Note that deviations from the jellium series occur for most heteroatom combinations. [b] Abundance maxima specified as a range indicate that there are no major differences in ion signal among the clusters listed (subsequent dramatic reduction).

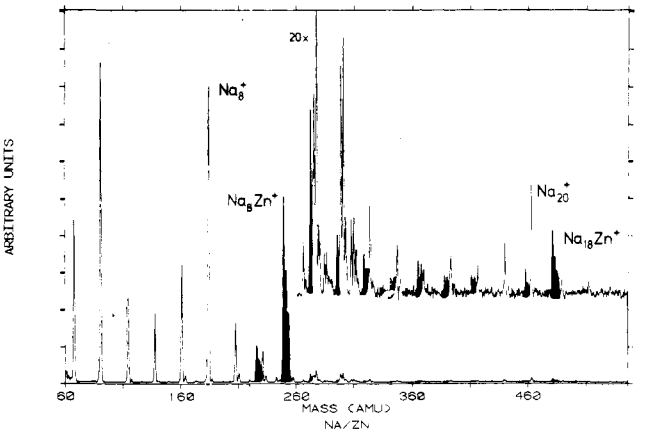

Figure 8. Photoionization mass spectrum obtained upon irradiating a Na/Zn cluster beam with the full output of a 1-kW Xe/Hg arc lamp. Clusters were generated by coexpansion of sodium and zinc metal vapors from a high-temperature oven at 1073 K. Cluster formation was enhanced by using a 0.6-mm diameter, 30° conical nozzle. The multimodal cluster ion abundances observed reflect abundance maxima among neutral sodium clusters (at Na_8 and Na_{20}, unshaded) and heteronuclear species containing one zinc atom (at Na_8Zn and $Na_{18}Zn$, shaded).

imum at M_nN^+). Figure 8 provides an example of such a measurement. In many cases, ionization potentials as well as ionization and fragmentation cross sections have not yet been obtained for the resulting species. Consequently the connection between ion abundance maximum and enhanced neutral stability is not clear-cut in each case. Nevertheless, measurements under various stagnation conditions suggest such a connection, and it appears that in most cases filling order reversals need to be postulated in order to explain deviations form the standard jellium approach.[190]

A chemical rationalization of these observations is that a centrally located heteroatom can induce (additional) structural anisotropy via interactions of its p, d, or f orbitals with the surrounding ligand shell. Concomitantly the barrier to large amplitude motion may be raised. For heteroclusters, steric effects would then still be important (as demonstrated by correlations of deviations in "magic" numbers with heteroatom radius) at temperatures for which bonding in fluxional *homonuclear* alkali clusters may be roughly approximated by assuming spherical symmetry.

With few exceptions (see 3.2) metal clusters must become rigid at low enough internal temperatures. Then total energy becomes a sensitive function of molecular geometry and packing. Calculations at various levels of sophistication both for small- and intermediate-sized (rigid) alkali clusters suggest that islands of enhanced thermodynamic stability deriving from dominant electronic terms in fluxional clusters may shift as the clusters are cooled below their melting transition.[77,191]

5. Summary and Outlook

The present status of experimental studies on neutral, gas-phase metal clusters can be summarized quite simply. We have available methods to make clusters of all metallic elements. However, particle fluxes are often very low, and the isomer and internal energy distributions produced are not known. Particle-specific information at this writing is limited to the following: (i) ionization potential and electron affinity measurements inconsistent with a metal/non-metal transition in a single cluster (except for group 2a and 2b metals), showing some element-specific quantum size effects below M_{10} but in general described purely in terms of classical electrostatics; (ii) electric deflection measurements on sodium and potassium clusters that have been interpreted in terms of almost cluster size invariant per atom polarizability and negligible static dipole moments; (iii) measurements for iron clusters suggesting that in clusters of ferromagnetic metals magnetic moment scales linearly with cluster size; (iv) band gap related measurements on copper cluster anions, which over the limited size range studied, have been interpreted to indicate that the gap may scale as $n^{-1.8}$; (v) not totally unambiguous chemical reactivity data, showing marked cluster size dependent variations in reaction rates and selectivity, which can be correlated with cluster ionization potentials for certain simple reactions involving electron transfer; (vi) spectroscopic studies on trimers of s-electron metals consistent with ground-state C_{2v} symmetry and in the case of homonuclear trimers providing classic examples of fluxionality as a result of dynamic Jahn–Teller distortions; (vii) many mass spectra that are a convolution of kinetic and thermodynamic effects associated with cluster production, ionization, and detection. There have been attempts particularly for alkali clusters to partially deconvolute these measurements and to make some inferences regarding relative thermodynamic stabilities leading to the application of global electronic structure models.

Future trends in this rapidly expanding research area will include (i) development of methods sensitive to cluster phase and internal temperature while still providing particle specificity, (ii) application of novel spectroscopic tools to structure determination and the characterization of isomer distributions in the size range below 20 atoms, (iii) systematic improvement and further development of cluster sources (high fluxes, colder clusters, production of purely thermodynamically controlled isomer distributions), (iv) generation of monodispersed neutral clusters in high-flux beams and characterization of chemical and physical properties

under truly particle-specific conditions, (v) characterization of cluster beam–surface interactions, and (vi) formation and study of monodispersed clusters on surfaces and in matrices. This effort will hopefully stimulate and ultimately require a generally applicable theoretical underpinning.

Acknowledgment. It is a pleasure and a privilege to acknowledge countless stimulating discussions with Prof. Ernst Schumacher. Much of the work discussed herein would not have been possible without the help and/or advice of my co-workers in Bern: R. Kunz, H.-P. Härri, K. Marti, P. Radi, M. Schär, and C. Yeretzian. I am grateful to the Swiss National Science Foundation for providing financial support during my time in Bern.

6. References

(1) Hoare, M. *Adv. Chem. Phys.* **1979**, *40*, 49.
(2) Mühlschlegel, B. In *Percolation, Localisation and Superconductivity*; Goldman, A., Wolf, S., Eds.; Nato ASI Series B 109; Plenum: New York, 1984. Parenboom, J.; Wyder, P.; Meier, F. *Phys. Rep.* **1981**, *78*, 173.
(3) Sinanoglu, O. *Chem. Phys. Lett.* **1981**, *81*, 188.
(4) Particularly in the case of group 2b clusters, where we expect a non-metal/metal transition to occur above about M_{40}. See 4.5.
(5) Vargaftik, M.; Zagorodnikov, V.; Stolyarov, I.; Moiseev, I.; Likholobov, V.; Kochubey, D.; Chuvilin, A.; Zaikovsky, VV.; Zamaeaev, K.; Timofeeva, G. *J. Chem. Soc., Chem. Commun.* **1985**, 937.
(6) Ceriotti, A.; Chini, P.; Della Pergola, R.; Longoni, G. *Inorg. Chem.* **1983**, *22*, 1595. See also: Chini, P. *J. Organomet. Chem.* **1980**, *200*, 37.
(7) See for example: Teo, B. *Inorg. Chem.* **1984**, *23*, 1251. Stone, A. *Inorg. Chem.* **1981**, *20*, 563. Minogs, D. *J. Chem. Soc., Chem. Commun.* **1983**, 706. Chini, P. *J. Organomet. Chem.* **1980**, *200*, 37. Teo, B.; Sloane, N. *Inorg. Chem.* **1986**, *25*, 2315. Mingos, D. *Chem. Soc. Rev.* **1986**, *15*, 31.
(8) Muetterties, E.; Krause, M. *Angew. Chem.* **1983**, *95*, 135. Muetterties, E.; Rhodin, T.; Band, E.; Brucker, C.; Petzer, W. *Chem. Rev.* **1979**, *79*, 91.
(9) Schmid, G. *Struct. Bonding (Berlin)* **1985**, *62*, 51.
(10) Pronk, B.; Brom, H.; de Jongh, L.; Longoni, G.; Ceriotti, A. *Solid State Commun.* **1986**, *59*, 349.
(11) Salahub, D. *Proceedings of the International Symposium on the Physics and Chemistry of Small Clusters*; Jena, P., Ed.; Wiley: New York, 1987.
(12) Cox, D.; Trevor, D.; Whetten, R.; Rohlfing, E.; Kaldor, A. *Phys. Rev. B* **1985**, *32*, 7290.
(13) This is an indication that there must be a discontinuous, entropically driven magnetic phase transition at intermediate cluster size—perhaps corresponding to the dimensions of several ferromagnetic domains.
(14) Note that the observation of measurable deflections implies that iron clusters produced by laser vaporization may have well-defined electronic states (rigid clusters) on the time scale of passage through the Stern–Gerlach magnet: Kaldor, A.; Cox, D.; Trevor, D.; Zakin, M. *Z. Phys. D* **1986**, *3*, 195.
(15) Schmidt, L.; Luss, D. *J. Catal.* **1971**, *22*, 269. Ertl, G. *Surf. Sci.* **1985**, *152*, 328.
(16) Harris, P. *Nature (London)* **1986**, *323*, 792.
(17) Zakin, M.; Brickman, R.; Cox, D.; Reichmann, K.; Trevor, D.; Kaldor, A. *J. Chem. Phys.* **1986**, *85*, 1198.
(18) Smalley, R. personal communication.
(19) Gor'kov, L.; Eliashberg, G. *Sov. Phys.—JETP (Engl. Transl.* **1965**, *21*, 940.
(20) Almloef, J. Proceedings of the 3'me Cycle School on Computational Chemistry, Chateau-d'Oex, 1986.
(21) Pettersson, L.; Bauschlicher, C., Jr. *Chem. Phys. Lett.* **1986**, *130*, 111.
(22) Very recently Be_{51} and Be_{57} have also been calculated at an ab initio level with predetermined structures. Computing time on a Cray X-MP was on the order of 3 h for both molecules: Ross, R.; Ermler, W.; Pitzer, R.; Kern, W. *Chem. Phys. Lett.* **1987**, *134*, 115.
(23) Boudart, M.; Aldag, A.; Ptak, L.; Benson, J. *J. Catal.* **1968**, *11*, 35. Bond, G. *Surf. Sci.* **1985**, *156*, 966.
(24) Boudart, M. *J. Mol. Catal.* **1985**, *30*, 27.
(25) Borel, J. *Surf. Sci.* **1981**, *106*, 1.
(26) Spencer, M. *Nature (London)* **1986**, *323*, 685.
(27) Whetten, R.; Cox, D.; Trevor, D.; Kaldor, A. *Surf. Sci.* **1985**, *156*, 8.
(28) Kaldor, A.; Cox, D.; Zakin, M., submitted for publication.
(29) Geusic, M.; Morse, M.; Smalley, R. *J. Chem. Phys.* **1985**, *82*, 590. Whetten, R.; Cox, D.; Trevor, D.; Kaldor, A. *Phys. Rev. Lett.* **1985**, *54*, 1494. Richtsmeier, S.; Parks, E.; Liu, K.; Pobo, K.; Riley, S. *J. Che.m Phys.* **1985**, *82*, 3659.
(30) Whetten, R.; Zakin, M.; Cox, D.; Trevor, D.; Kaldor, A. *J. Chem. Phys.* **1986**, *85*, 1697.
(31) Cox, D.; Trevor, D.; Zakin, M.; Kaldor, A. *Proceedings of the International Symposium on the Physics and Chemistry of Small Clusters*; Jena, P., Ed.; Wiley: New York, 1987.
(32) Ozin, G. *Faraday Symp., Chem. Soc.* **1980**, *14*, 7.
(33) Wallenberg, L.; Petford-Long, A.; Bovin, J.; Smith, D.; Long, N. *Proceedings of the International Symposium on the Physics and Chemistry of Small Clusters*; Jena, P., Ed.; Wiley: New York, 1987.
(34) Steeb, S., Warlimont, Eds. *Rapidly Quenched Metals*; North-Holland: Amsterdam, 1985.
(35) Schechtman, D.; Blech, I.; Gratias, D.; Cahn, J. *Phys. Rev. Lett.* **1984**, *53*, 1951. Levine, D.; Steinhardt, P. *Phys. Rev. Lett.* **1984**, *53*, 2477. Nelson, D.; Halperin, B. *Science (Washington, D.C.)* **1985**, *229*, 223. Dubost, B.; Lang, J.-M.; Tanaka, M.; Sainfort, P.; Audier, M. *Nature (London)* **1986**, *324*, 48.
(36) Ringger, M.; Corb, B.; Hidber, H.; Schlogl, R.; Wiesendanger, R.; Stemmer, A.; Rosenthaler, L.; Brunner, A.; Oelhafen, P.; Güntherodt, H.-J. *IBM J. Res. Dev.* **1986**, *30*, 500. Also: Güntherodt, H.-J. Proceedings of the Sixth International Conference on Amorphous Metals, Garmisch-Partenkirchen, 1986.
(37) Zintl, E. *Angew. Chem.* **1939**, *52*, 1.
(38) Rizzo, T.; Park, Y.; Levy, D. *J. Am. Chem. Soc.* **1985**, *107*, 277.
(39) Fenn, J. Proceedings of the Tenth International Symposium on Molecular Beams, Cannes, 1985.
(40) Vaida, V.; Cooper, N.; Hemley, R.; Leopold, D. *J. Am. Chem. Soc.* **1981**, *103*, 7022. Leutwyler, S.; Even, U. *Chem. Phys. Lett.* **1981**, *84*, 188. Leutwyler, S.; Even, U.; Jortner, J. *J. Phys. Chem.* **1981**, *85*, 3026.
(41) Largest cluster ions formed in this fashion have been M_4^+; see: Hollingsworth, W.; Vaida, V. *J. Phys. Chem.* **1986**, *90*, 1235. Frey, H.; Irlet, T.; Kappes, M.; Schumacher, E., to be submitted for publication.
(42) Kappes, M.; Leutwyler, S. In *Atomic and Molecular Beam Methods*; Scoles, G., Ed.; Oxford University: Oxford, 1987; Vol. 1.
(43) Wöste, L. Ph.D. Thesis, University of Bern, 1978.
(44) Okumura, Y.; Horiike, H.; Mizuhashi, K. *Rev. Sci. Instrum.* **1984**, *55*, 1.
(45) Jarrold, M.; Bower, J. *J. Chem. Phys.* **1986**, *85*, 5373.
(46) Leopold, D.; Ho, J.; Lineberger, W. *J. Chem. Phys.* **1987**, *86*, 1715.
(47) Fayet, P.; McGlinchey, M.; Wöste, L. *J. Am. Chem. Soc.* **1987**, *109*, 1733. Wöste, L. personal communication.
(48) Zheng, L.; Brucat, P.; Petiette, C.; Yang, S.; Smalley, R. *J. Chem. Phys.* **1985**, *83*, 4273. Fayet, P.; Woste, L. *Z. Phys. D* **1986**, *3*, 177.
(49) Knight, W.; Monot, R.; Dietz, E.; George, A. *Phys. Rev. Lett.* **1978**, *40*, 1324.
(50) de Heer, W.; George, A.; Gerber, W.; Knight, W., unpublished results.
(51) Hoffman, M. Ph.D. Thesis, University of Bern, 1980.
(52) Cox, D.; Trevor, D.; Whetten, R.; Rohlfing, E.; Kaldor, A. *J. Chem. Phys.* **1986**, *84*, 4651.
(53) Knight, W.; Clemenger, K.; de Heer, W.; Saunders, W. *Phys. Rev. B* **1985**, *31*, 2539.
(54) Altman, R.; Schumacher, E., to be submitted for publication.
(55) Frisch, O. *Z. Phys.* **1933**, *86*, 42.
(56) Herrmann, A.; Leutwyler, S.; Wöste, L.; Schumacher, E. *Chem. Phys. Lett.* **1979**, *62*, 444.
(57) Buck, U.; Meyer, H. *Phys. Rev. Lett.* **1984**, *52*, 109.
(58) Kappes, M.; Yeretzian, C.; Vayloyan, A.; Schumacher, E. to be submitted for publication.
(59) Bowles, R.; Park, S.; Otsuka, N.; Andres, R. *J. Mol. Catal.* **1983**, *20*, 279.
(60) Arnold, M.; Kowalski, J.; zu Putlitz, G.; Stehlin, T.; Träger, F. *Z. Phys. A* **1985**, *322*, 179.
(61) Abshagen, M.; Arnold, M.; Kowalski, J.; Meyberg, M.; zu Putlitz, G.; Stehlin, T.; Träger, F.; Well, J. *Proceedings of the International Symposium on the Physics and Chemistry of Small Clusters*; P, Jena, Ed.; Wiley: New York, 1987.
(62) Fayet, P.; Granzer, F.; Hegenbart, G.; Moisar, E.; Pischel, B.; Wöste, L. *Phys. Rev. Lett.* **1985**, *55*, 3002.
(63) Arnold, M.; Kowalski, J.; zu Putlitz, G.; Stehlin, T.; Träger, F. *Surf. Sci.* **1985**, *156*, 149. Pflaum, R.; Sattler, K.; Recknagel, E. *Z. Phys. D* **1986**, *1*, 131.
(64) Clemenger, K. Ph.D. Thesis, University of California at Berkeley, 1985.
(65) Dreyfuss, D.; Wachmann, H. *J. Chem. Phys.* **1982**, *76*, 2031.
(66) Superconducting bolometric techniques while extensively applied to the detection of, and internal excitation measure-

ment in, van der Waals clusters have yet to be utilized for metal cluster beams.
(67) Rohlfing, E.; Valentini, J. *Chem. Phys. Lett.* **1986**, *126*, 113.
(68) It is not clear whether larger metal clusters have measurable fluorescence yields due to extremely short excited-state lifetimes.[164]
(69) Kappes, M.; Kunz, R.; Schumacher, E. *Chem. Phys. Lett.* **1982**, *91*, 413.
(70) Ketkar, S. N., Extrel Corp., submitted for publication.
(71) Thum, F.; Hofer, W. *Surf. Sci.* **1979**, *90*, 331. Staudenmeier, G.; Hofer, W.; Liebl, H. *Int. J. Mass Spectrom. Ion Phys.* **1976**, *11*, 103. Beuhler, R.; Friedman, L. *Nucl. Instrum. Methods* **1980**, *170*, 309.
(72) Knight, W.; Clemenger, K.; de Heer, W.; Saunders, W.; Chou, M.; Cohen, M. *Phys. Rev. Lett.* **1984**, *52*, 2141.
(73) In photoionization studies on s-electron metal clusters dramatically multimodal ion distributions have been connected with "magic" electron counts in the precursor neutrals (see 4.6(ii) and 4.7).[72] There are several pieces of circumstantial evidence that tend to rule out "magic" ionization cross sections as routes to these maxima: (i) dependence of alkali mass spectra on source stagnation pressure;[72,144,196] (ii) K_x^+ mass spectra obtained under conditions such that they reflect positive ion stabilities rather than neutral abundances, showing ion abundance maxima shifted up one atom from typical photoionization measurements;[195,196] (iii) sputtering studies on Cu, Ag, and Au targets that yield cluster cations and anions whose stability-related particle size distributions also manifest maxima shifted up or down by one atom relative to the series found for neutral alkalis.[181]
(74) Kappes, M.; Schär, M.; Vayloyan, A.; Heiz, U.; Schumacher, E. to be submitted for publication.
(75) Herrmann, A. Ph.D. Thesis, University of Bern, 1978.
(76) Kappes, M.; Schär, M.; Schumacher, E.; Vayloyan, A. *Z. Phys. D.* **1987**, *5*, 359.
(77) Kouetecky, J.; Fantucci, P. *Chem. Rev.* **1986**, *86*, 539. Koutecky, J., private communication.
(78) Wülfert, S.; Herren, D.; Leutwyler, S. *J. Chem. Phys.* **1987**, *86*, 3751.
(79) Barnes, J.; Gough, T. *Chem. Phys. Lett.* **1986**, *130*, 297.
(80) Gough, T.; Knight D.; Scoles, G. *Chem. Phys. Lett.* **1983**, *97*, 155.
(81) Ray, D.; Robinson, R.; Gwo, D.; Saykally, R. *J. Chem. Phys.* **1986**, *84*, 1171.
(82) Luijks, C.; Stolte, S.; Reuss, J. *Chem. Phys.* **1981**, *62*, 217.
(83) See for example: Carnovale, F.; Peel, J.; Rothwell, R. *Proceedings of the International Symposium on the Physics and Chemistry of Small Clusters*; Jena, P., Ed.; Wiley: New York, 1987.
(84) Legon, A.; Millen, D. *Chem. Rev.* **1986**, *86*, 635.
(85) Hayden, J.; Woodward, R.; Gole, J. *J. Phys. Chem.* **1986**, *90*, 1799. Gole, J.; Green, G.; Pace, S.; Preuss, D. *J. Chem. Phys.* **1982**, *76*, 2247.
(86) Zheng, L.; Karner, C.; Brucat, P.; Yang, S.; Petiette, C.; Craycraft, M.; Smaller, R. *J. Chem. Phys.* **1986**, *85*, 1681.
(87) Brucat, P.; Zheng, L.; Petiette, C.; Yang, S.; Smalley, R. *J. Chem. Phys.* **1986**, *84*, 3078.
(88) Delacretaz, G.; Grant, E.; Whetten, R.; Wöste, L.; Zwanziger, J. *Phys. Rev. Lett.* **1986**, *56*, 2598. Broyer, M.; Delacretaz, G.; Labastie, P.; Wolf, J.; Wöste, L. *Phys. Rev. Lett.* **1986**, *57*, 1851.
(89) Herrmann, A.; Leutwyler, S.; Schumacher, E.; Wöste, L. *Chem. Phys. Lett.* **1979**, *62*, 216.
(90) Wöste, L., personal communication.
(91) Engelke, F., personal communication.
(92) Shim, I.; Gingerich, K. *J. Chem. Phys.* **1982**, *77*, 2490.
(93) Morse, M.; Hopkins, J.; Langridge-Smith, P.; Smalley, R. *J. Chem. Phys.* **1983**, *79*, 5316.
(94) Kappes, M.; Schär, M.; Schumacher, E. to be submitted for publication.
(95) In classical descriptions of total energy (surface + volume term) for spherical metal clusters, fragmentation via monomer loss is thermodynamically favored over scission.[138] Ab initio calculations on alkali clusters come to similar conclusions (with exceptions occurring near stability islands). While we have little data on photodissociation or collisional dissociation of neutral metal clusters, there are many such measurements for cluster ions. These data are generally consistent with sequential monomer vaporization.
(96) Wang, P.; Ansermet, J.-P.; Rudaz, S.; Whang, Z.; Shore, S.; Schlichter, C.; Sinfelt, J. *Science (Washington, D.C.)* **1986**, *234*, 35.
(97) Sako, S. *Proceedings of the International Symposium on the Physics and Chemistry of Small Clusters*; Jena, P., Ed.; Wiley: New York, 1987.
(98) See for example: Gingerich, K. In *Current Topics in Materials Science*; Kaldis, E., Ed.; North-Holland: Amsterdam, 1980; Vol. 6.
(99) Wallenberg, L.; Bovin, J.; Schmid, G. *Surf. Sci.* **1985**, *156*, 256. Smith, D.; Petford-Long, A.; Wallenber_, L.; Bovin, J. *Science (Washington, D.C.)* **1986**, *233*, 872. Iijima, S.; Ichihashi, T. *Phys. Rev. Lett.* **1986**, *56*, 616.
(100) Sattler, K. *Proceeding of the International Symposium on the Physics and Chemistry of Small Clusters*, Jena, P., Ed.; Wiley: New York, 1987.
(101) Bartell, L. *Chem. Rev.* **1986**, *86*, 491.
(102) De Boer, B.; Stein, G. *Surf. Sci.* **1981**, *106*, 84.
(103) Torchet, G.; Bouchier, H.; Farges, J.; de Faraudy, M.; Roault, B. *J. Chem. Phys.* **1984**, *81*, 2137.
(104) Montano, P., personal communication.
(105) Cox, D.; Trevor, D.; Kaldor, A., submitted for publication.
(106) Peterson, K.; Dao, P.; Castleman, A., Jr. *J. Chem. Phys.* **1983**, *79*, 777. Dao, P.; Peterson, K.; Castleman, A., Jr. *J. Chem. Phys.* **1984**, *80*, 563. Rothe, E.; Sinha, D.; Ranjbar, F. *J. Chem. Phys.* **1982**, *76*, 5650.
(107) A multiple expansion cluster sources (MECS[197]) providing broad (±20-atom) size distributions of large clusters was used in these experiments: R., Kunz, E., Schumacher, unpublished results.
(108) Schulz, C.; Haugstatter, H.; Tittes, H.; Hertel, I. *Phys. Rev. Lett.* **1986**, *57*, 1703.
(109) Kappes, M.; Schär, M.; Heiz, U.; Schumacher, E., to be submitted for publication.
(110) Hanley, L.; Anderson, S. *Chem. Phys. Lett.* **1985**, *122*, 410.
(111) Armentrout, P.; Loh, S.; Ervin, K. *J. Am. Chem. Soc.* **1984**, *106*, 1161.
(112) Freas, R.; Campana, J. *J. Am. Chem. Soc.* **1985**, *107*, 6202.
(113) Jacobsen, D.; Freiser, B. *J. Am. Chem. Soc.* **1986**, *108*, 27.
(114) Reents, W., Jr.; Mandich, M.; Bondybey, V. *Chem. Phys. Lett.* **1986**, *131*, 1. Mandich, M.; Bondybey, V.; Reents, W. *J. Chem. Phys.* **1987**, *86*, 4245.
(115) Alford, J.; Williams, P.; Trevor, D.; Smalley, R. *Int. J. Mass Spec. Ion Proc.* **1986**, *72*, 33.
(116) Castleman, A., Jr.; Keesee, R. *Z. Phys. D* **1986**, *3*, 167.
(117) Jarrold, M.; Bower, J.; Kraus, J. *J. Chem. Phys.* **1987**, *86*, 3876.
(118) Garland, D.; Lindsay, D. *J. Chem. Phys.* **1983**, *78*, 2813.
(119) Lindsay, D.; Thompson, G. *J. Chem. Phys.* **1982**, *77*, 1114.
(120) Thompson, G.; Lindsay, D. *J. Chem. Phys.* **1981**, *74*, 959.
(121) Weltner, W., Jr.; van Zee, R. *Ann. Rev. Phys. Chem.* **1984**, *35*, 291.
(122) Morse, M. *Chem. Rev.* **1986**, *86*, 1049.
(123) Broyer, M.; Delacretaz, G.; Labastie, P.; Wolf, J.; Wöste, L. *J. Phys. Chem.* **1987**, *91*, 2626.
(124) Radi, P. Ph.D. Thesis, University of Bern, 1986.
(125) Radi, P.; Kappes, M.; Schumacher, E. *Chem. Phys. Lett.*, to be submitted for publication.
(126) Zwanziger, J.; Whetten, R.; Grant, E. *J. Phys. Chem.* **1986**, *90*, 3298.
(127) For example the melting point of 25-Å diameter gold particles has been shown to lie below 800 K, and smaller particles are thought to have even lower melting points—note that melting is thought to begin at the metal surface[128] and that the concept of melting itself becomes progressively less well defined the smaller the particle size[192] (see below); furthermore, certain very small clusters undergo large-particle motion large enough to fulfill the Lindemann criterion for melting[193] (i.e. >10% root-mean-square fluctuations in bond lengths) even in their vibrational ground state (below).
(128) Pietronero, L.; Tosatti, E. *Solid State Commun.* **1979**, *32*, 255.
(129) Jellinek, J.; Beck, T.; Berry, R. *J. Chem. Phys.* **1986**, *84*, 2783. Amar, F.; Berry, R. *J. Chem. Phys.* **1986**, *85*, 5943.
(130) Berry, R. *Proceedings of the International Symposium on the Physics and Chemistry of Small Particles*; Jena, P., Ed.; Wiley: New York, 1987.
(131) Note however: Eichenauer, D.; Le Roy, R. *Phys. Rev. Lett.* **1986**, *57*, 2920. Leutwyler, S.; Boesiger, J. *Phys. Rev. Lett.* **1987**, *59*, 1895.
(132) See for example: Kroto, H.; Heath, J.; O'Brien, S.; Curl, R.; Smalley, R. *Nature (London)* **1985**, *318*, 162.
(133) Buffat, R. *Thin Solid Films* **1976**, *32*, 283.
(134) Solliard, C.; Flueli, M. *Surf. Sci.* **1985**, *156*, 487.
(135) Kip, B.; Duivenvoorden, F.; Koningsberger, D.; Prins, R. *J. Am. Chem. Soc.* **1986**, *108*, 5633.
(136) Riley, S. *Proceedings of the International Symposium on the Physics and Chemistry of Small Particles*; Jena, P., Ed.; Wiley: New York, 1987.
(137) See for example: Herrmann, A.; Leutwyler, S.; Schumacher, E.; Wöste, L. *Chem. Phys. Lett.* **1977**, *52*, 418.
(138) Klots, C. *J. Chem. Phys.* **1985**, *83*, 5854; *Z. Phys. D* **1987**, *5*, 83.
(139) Kappes, M.; Schär, M.; Schumacher, E. *J. Phys. Chem.* **1987**, *91*, 658.
(140) Gspann, J. *Z. Phys. D* **1986**, *3*, 143.
(141) Shimoda, K. *Top. Appl. Phys.* **1976**, *13*, 11.
(142) Schär, M. Diploma Thesis, University of Bern, 1984.
(143) Herrmann, A.; Schumacher, E.; Wöste, L. *J. Chem. Phys.* **1978**, *68*, 2327.

(144) Kappes, M.; Schär, M.; Radi, P.; Schumacher, E. *J. Chem. Phys.* **1986**, *84*, 1863.
(145) Saunders, W. *SPIE* **1986**, *620*, 46.
(146) Hoareau, A.; Cabaud, B.; Melinon, P. *Surf. Sci.* **1981**, *106*, 195.
(147) Rohlfing, E.; Cox, D.; Kaldor, A.; Johnson, K. *J. Chem. Phys.* **1984**, *81*, 3846.
(148) Saito, Y.; Yamauchi, K.; Mihama, K.; Noda, T. *Jpn. J. Appl. Phys.* **1982**, *21*, L396.
(149) Walstedt, R.; Bell, R. *Phys. Rev. A* **1986**, *33*, 2830.
(150) Powers, D.; Hansen, S.; Geusic, M.; Michalopoulos, D.; Smalley, R. *J. Chem. Phys.* **1983**, *78*, 2866.
(151) Cox, D.; Kaldor, A., to be submitted for publication.
(152) Bowen, K., personsal communication.
(153) See for example: Leutwyler, S.; Heinis, T.; Jungen, M. *J. Chem. Phys.* **1982**, *76*, 4290.
(154) Heiz, U. Diploma Thesis, University of Bern, 1987. Delacretaz, G. Ph.D. Thesis, Ecole Polytechnique Federale de Lausanne, 1985.
(155) Brechignac, C.; Cahuzac, P. *Z. Phys. D* **1986**, *3*, 121.
(156) Saunders, W.; Clemenger, K.; de Heer, W.; Knight, W. *Phys. Rev. B* **1985**, *32*, 1366.
(157) Peterson, K.; Dao, P.; Farley, R.; Castleman, A., Jr. *J. Chem. Phys.* **1984**, *80*, 1780.
(158) Kappes, M.; Schär, M.; Röthlisberger, U.; Yeretzian, C.; Schumacher, E. *Chem. Phys. Lett.* **1988**, *143*, 251.
(159) Wood, D. *Phys. Rev. Lett.* **1981**, *46*, 749. Smith, J. *AIAA J.* **1965**, *3*, 648.
(160) Nitzan, A. *J. Chem. Phys.*, to be submitted for publication. See also: van Staveren, M.; Brom, H.; de Jongh, L.; Ishii, Y. *Phys. Rev. B* **1987**, *35*, 7749.
(161) Surface tension and compressibility values are taken for liquid metals at their respective melting points. Equation 5 results from the assumption that $\ln (V_x/V_\infty) = -2\kappa\sigma/R_x$ where V_x and V_∞ are atomic volumes in cluster and bulk, respectively. It must be solved iteratively. Details can be found in ref 143 and 144.
(162) *Handbook of Chemistry and Physics*, 60th ed.; CRC: Boca Raton, 1980.
(163) Plieth, W. *Surf. Sci.* **1985**, *156*, 530.
(164) Cheshnovsky, O.; Brucat, P.; Yang, S.; Pettiette, C.; Craycraft, M.; Smalley, R. *Proceedings of the International Symposium on the Physics and Chemistry of Small Clusters*; Jena, P., Ed.; Wiley: New York, 1987.
(165) Kubo, R. *J. Phys. Soc. Jpn.* **1962**, *17*, 975.
(166) Wood, D.; Ashcroft, N. *Phys. Rev. B* **1982**, *25*, 6255.
(167) Schär, M.; Vayloyan, A.; Kappes, M.; Schumacher, E., to be submitted for publication.
(168) Snider, D.; Sorbello, R. *Surf. Sci.* **1984**, *143*, 204.
(169) Brechignac, C.; Broyer, M.; Cahuzac, P.; Delacretaz, G.; Labastie, P.; Wöste, L. *Chem. Phys. Lett.* **1985**, *120*, 559.
(170) Brechignac, C., personal communication.
(171) Kappes, M.; Radi, P.; Schär, M.; Yeretzian, C.; Schumacher, E. *Z. Phys. D* **1986**, *3*, 113.
(172) There are several apparent exceptions to this rule: Bi_x, Sb_x, and mixed clusters thereof. Conceivably this is a function of weaker per atom binding energies than generally encountered for transition metals: Wheeler, R.; Laihing, K.; Wilson, W.; Duncan, M. *Chem. Phys. Lett.* **1986**, *113*, 8. Wheeler, R.; Laihing, K.; Wilson, W.; Allen, J.; King, R.; Duncan, M. *J. Am. Chem. Soc.* **1986**, *108*, 8101.
(173) Note that the first study contained a rough approximation of terminal seed gas temperature *without* sodium present; in the later study this was mistakenly interpreted to be a temperature assessment for resultant sodium clusters.
(174) Mass spectra identical with those obtained in the later sodium-seeded beam study can be produced by neat sodium vapor expansion where molten clusters are likely produced.[139] Is it possible that the first measurement probed *colder* clusters and that differences are due to incipient packing stabilisation effects (see 4.8)?
(175) Knight, W.; de Heer, W.; Clemenger, K.; Saunders, W. *Solid State Commun.* **1985**, *53*, 445.
(176) Kappes, M.; Schär, M., unpublished results.
(177) Martins, J.; Car, R.; Buttet, J. *Surf. Sci.* **1981**, *106*, 265. Ekardt, W. *Phys. Rev. B* **1984**, *29*, 1558. Beck, D. *Solid State Commun.* **1984**, *49*, 381. Chou, M.; Cleland, A.; Cohen, M. *Solid State Commun.* **1984**, *52*, 645.
(178) Mayer, M.; Jensen, J. *Elementary Theory of Nuclear Shell Structure*; Wiley: New York, 1955.
(179) Knight, W.; de Heer, W.; Saunders, W. *Z. Phys. D* **1986**, *3*, 109.
(180) Clemenger, K. *Phys. Rev. B* **1985**, *32*, 1359.
(181) Katakuse, I.; Ichihara, I.; Fujita, Y.; Matsuo, T.; Sukurai, T.; Matsuda, H. *Int. J. Mass Spectrom. Ion Phys.* **1985**, *67*, 229; *Ibid.* **1986**, *74*, 33.
(182) Begemann, W.; Meiwes-Broer, K.; Lutz, H. *Phys. Rev. Lett.* **1986**, *56*, 2248.
(183) Philipps, J. *Chem. Rev.* **1986**, *86*, 619.
(184) Upton, T. *Phys. Rev. Lett.* **1986**, *56*, 2168.
(185) Knight, W.; de Heer, W.; Saunders, W.; Clemenger, K.; Chou, M.; Cohen, M. *Chem. Phys. Lett.* **1987**, *134*, 1.
(186) Martins, J.; Buttet, J.; Car, R. *Phys. Rev. Lett.* **1984**, *53*, 655; *Phys. Rev. B* **1985**, *31*, 1804.
(187) Cohen, M.; Chou, M.; Knight, W.; de Heer, W. *J. Phys. Chem.* **1987**, *91*, 3141.
(188) Kappes, M.; Schär, M.; Radi, P.; Schumacher, E. *Chem. Phys. Lett.* **1985**, *119*, 11.
(189) Kappes, M.; Schar, M.; Yeretzian, C.; Heiz, U.; Vayloyan, A.; Schumacher, E. *Proceedings of the International Symposium on the Physics and Chemistry of Small Clusters*; Jena, P., Ed.; Wiley: New York, 1987.
(190) Yeretzian, C. Diploma Thesis, University of Bern, Bern, 1985.
(191) See for example: Manninen, M. *Solid State Commun.* **1986**, *59*, 281; *Phys. Rev. B* **1986**, *34*, 6886; Reference 198.
(192) Etters, R.; Kaelberer, J. *J. Chem. Phys.* **1977**, *66*, 5112. Berry, R.; Jellinek, J.; Natanson, G. *Phys. Rev. A* **1984**, *30*, 919. Natanson, G.; Amar, F.; Berry, R. *J. Chem. Phys.* **1983**, *78*, 399. Berry, R.; Jellinek, J.; Natanson, G. *Chem. Phys. Lett.* **1984**, *107*, 227.
(193) See for example: Kaelberer, J.; Etters, R. *J. Chem. Phys.* **1977**, *66*, 3233.
(194) Meckstroth, W.; Ridge, D.; Reents, W., Jr. *J. Phys. Chem.* **1986**, *89*, 612.
(195) Brechignac, C.; Cahuzac, P. *Proceedings of the International Symposium on the Physics and Chemistry of Small Clusters*; Jena, P., Ed.; Wiley: New York, 1987.
(196) Brechignac, C.; Cahuzac, P.; Roux, J. *J. Chem. Phys.* **1987**, *87*, 229.
(197) Bowles, R.; Kolstad, J.; Calo, J.; Andres, R. *Surf. Sci.* **1981**, *106*, 117.
(198) Wang, Y.; George, T.; Lindsay, D.; Beri, A. *J. Chem. Phys.* **1987**, *86*, 3493.
(199) Kappes, M.; Radi, P.; Schär, M.; Schumacher, E. *Chem. Phys. Lett.* **1985**, *113*, 243.